Version of Record: https://www.sciencedirect.com/science/article/pii/S235271022201587X
Manuscript_8658446320b3470f8543eb7127eba8d9

Eco-Friendly and Cost-Effective Self-Compacting Concrete Using Waste Banana Leaf Ash

Nusrat Jahan Mim[1], Md Montaseer Meraz[1], Md. Hamidul Islam[1], Ehsan Noroozinejad Farsangi[2,3]*, Md. Tanjid Mehedi[1], Sk. Abdul Kader Arafin[4], Rajesh Kumar Shrestha[5]

[1]Department of Building Engineering & Construction Management, Khulna University of Engineering & Technology (KUET), Khulna - 9203, Bangladesh.

[2] Department of Civil Engineering, The University of British Columbia (UBC), Vancouver, BC, Canada

[3] The International Institute for Urban Systems Engineering, Southeast University, Jiangsu, China

[4]Department of Physics, Daffodil International University, Dhaka, Bangladesh.

[5]Department of Civil Engineering, Tribhuvan University, Institute of Engineering, Thapathali Campus, Kathmandu, Nepal

ehsan.noroozinejad@ubc.ca (***Corresponding Author**)

ORCID: https://orcid.org/0000-0002-2790-526X

Abstract

The requirements of higher cement content and numerous admixtures in Self-Compacting Concrete (SCC) yields a comparatively high production due to the high cement consumption that limits its use in everyday construction. As a result, it is prudent to consider alternatives for decreasing the environmental effects while producing a cost-effective SCC. Therefore, this study aims to investigate the fresh mechanical, durability, and microstructural characteristics as well as the environmental impacts of self-compacting concrete (SCC) incorporating waste banana leaf ash (BLA) to determine the optimum percentage of BLA. Concrete mixtures with a 10%, 20%, and 30% OPC substitutions were investigated. The test findings revealed that all the fresh mixes performed within the EFNARC (2002) recommended limit. Despite the fact that increasing concentrations of BLA reduced the mechanical properties, concentrations of up to 20% BLA demonstrated strength comparable to the control mix. Furthermore, choloride ion penetration increased to 4%, with 20% BLA replacement falling into the moderate ion permeability zone. Finally, a relatively lower CO_2-eq (maximum 29.13% reduction) per MPa indicate a significant positive impact due to the reduced Global Warming Potential (GWP).

Keywords: *Self-Compacting Concrete (SCC), low-cost SCC, Waste banana leaf ash, Workability, Hardened properties.*

1. Introduction

The most important prerequisite for any country's total development is sufficient housing, roadways, bridges, and other civil engineering infrastructures [1]. Concrete is widely acknowledged as the world's most essential building material and has traditionally been utilized extensively in infrastructural development [2]. Although becoming a major part of a national growth, the construction materials industry consumes the most natural resources. Infrastructure projects and building construction process consume 60% of all lithosphere raw materials [3, 4]. It is the third-largest CO_2-emitting manufacturing industry in the world, contributing roughly 5 to 10% of the global CO_2 emissions, especially concrete manufacturing accounted for the majority among this pollution [5, 6]. For that reason, environmentally friendly construction materials are essential.

Self-compacting concrete (SCC) is a form of concrete featuring minimal flow resistance which enables this to be placed and compacted by its own weight without the need for vibration but still possessing enough viscosity for the prevention of segregation as well as bleeding [7-9]. It may flow and solidify into the molds inside the rebar without causing vibrations for its high flowability [10]. That characteristic makes it feasible for placing the concrete into difficult building situations, such as seismic zones having crowded reinforcement [11]. But it has additional expense for having excessive powder content and admixtures, as well as large quantities of Cementitious materials [12]. The substantial cement content often involves a great deal of hydration heating, autogenous shrinkage, as well as huge cash. Additionally, cement production consumes huge energy about $7.36*10^6$ kJ per ton of cement [13] as well as has a significant environmental impact. As the demand for SCC is much higher for its high-performance characteristics, researchers are trying to use waste materials to make it more environmentally friendly [14, 15]. Numerous authors have explored agricultural by-products, including tobacco waste ash, sugar cane straw ash, rice husk ash, egg-shell ash, palm oil fuel ash, groundnut shell ash, and other farmland by-products as a partial substitute for cement in concrete and discovered their possibilities as decent pozzolans and great prospects in concrete quality [16-21]

In recent times, the feasibility of Argo leftover ashes is generating a growing interest towards renewable and environmentally friendly sources as additional cementitious ingredients. According to ASTM C 125-13 [22], a pozzolan is a substance having siliceous and aluminous

chemical structure contains minimal to no cement. However, when it is finely divided and combined with water, calcium hydroxide is chemically reacted with it at room temperature to create composites possessing cement-like characteristics. Such viewpoints allow us to evaluate banana leaf ash (BLA) as pozzolanic material in concrete and mortar products [23] which is an agricultural waste that may be used as supplementary cementitious material in construction. Previously, almost 95 million tons of bananas and plantains were cultivated [24, 25], which means, approximately 10.22 million tons of production of banana plant ashes, globally [26].

There has been very few research conducted on the strength of conventional concrete by partially replacing cement with up to 30% BLA, and it has yet to be used as a supplemental cementing ingredient in SCC. Therefore, this study aims to investigate enabling the utilization of BLA in concrete. In the context of the utilization of SCC, the workability of combined with BLA as well as its mechanical and durability characteristics, are the most critical factors. Therefore, this paper evaluates the effect of BLA on the fresh, mechanical, durability, and microstructural performance of SCC at varied substitution rates. By lowering certain percentages of OPC, this study also aims to provide an appropriate mix design reference for eco-friendly self-compacting concrete. Finally, the environmental impact of the produced concrete was carried out to ensure its utilization in structurally sustainable applications.

1.1. Significance of the study

In this study, the tests were performed to determine whether the properties of SCC could be improved through incorporating banana leaf ash with it in variable concentrations. The demand for research on SCC is substantial as it offers high-performance characteristics. Researchers around the world are doing countless studies utilizing waste ingredients to create it more ecologically beneficial products. A large number of waste products, such as waste ceramic powders, palm oil fuel ash, synthetic fibers, fly ash, foundry sand waste, crumb rubber coconut shell aggregate, recycled aggregates, polypropylene fibers, rice husk ash, and others, have been used in SCC for replacing the coarse aggregate, fine aggregate, and cement partially. On the other hand, BLA has yet to be employed in SCC as a supplementary cementing ingredient. A banana tree can only yield fruits once over its whole life span. The tree is near useless once the fruits have been harvested. As a consequence,

banana leaf ash may be utilized as a low-cost partial replacement for cement as well as also reduce the Global Warming. So, the primary element to look for in this investigation is the engineering characteristics of these substitutes.

A pozzolan material is defined by ASTM C 125-13 [13] as a product that has chemical structure based on siliceous or siliceous and aluminous material, with little or no portions of cement but that will, in finely divided form and with water, it reacts chemically with calcium hydroxide at ordinary temperatures to form compounds that has cementitious properties. From these, banana leaf ash (BLA) was assessed as pozzolanic materials to be employed in cement mortars and normal concrete in previous studies [27, 28]. However, using BLA in SCC not only allows it to be employed in closely spaced reinforcing regions as well as segregation-resistant structures, but it also provides a more eco-friendly and cost-effective alternative.

2. Experimental program

2.1. Materials

In the entire experimental program, 52.5 grade Ordinary Portland Cement (OPC) type I complying with BS EN 197-1 [29], was used. For the supplementary cementing material, BLA, the banana leaves were collected from a local market and sun-dried for about 7 days. BLA was produced by burning at a reasonably high temp, with in range of 650 degrees Celsius, as well as the rate of burning was set to 10 degrees Celsius per minute in accordance with the recommendations found in the research conducted by Vayghan et al. [30]. The burnt ashes were kept at maximum heat for a total of 75 minutes. The ashes were taken out of the furnace after the retaining time elapsed, and it took less than five minutes for them to return to room temperature after being cooled down. After being passed through a 75 mm sieve opening, the BLA was deemed more desirable for the replacement of cement. The X-ray diffraction pattern of banana leaf ash (BLA) is depicted in Figure 1. XRD results demonstrated an amorphous phase of about 84.0%. The remaining crystalline phases were identified as calcite ($CaCO_3$), quartz (SiO_2), magnesium carbonate ($MgCO_3$). The crystalline forms were, most likely, originated due the slow cooling of the BLA inside the oven, because ash remained at temperatures of approximately 80 °C after burning until its removal from the oven after 8 h. However, XRD graph has a shifted peak when contents materials or vary temperature. The peaks on plane changed such as transfer to another degree, higher intensity,

lower intensity. As a result, this burning procedure could be improved for the industrial production of the pozzolan material.

The oxide composition of the BLA was determined using X-ray fluorescence spectrometer Epsilon1 operated at 40 kV and 18 mA. The current of the equipment was adjusted to a maximum value of 1 mA using a 10 mm collimator. A counting period of 100 s was adopted for all the measurements taken. The chemical composition BLA, in terms of the main oxides, were SiO_2 = 43.88%, Al_2O_3 = 5.38%, and Fe_2O_3 = 4.48%, and thus they met the requirements establishing a minimum content of 50% of these minerals as per ASTM C618 [31]. The loss on ignition was 5.02% which is close to the maximum stipulated limit (6%). Because of its nature and composition, the BLA was classified as class C according to ASTM C618 [31]. Figure 2 presents the OPC and BLA used in this study.

As fine aggregates, washed river sand from Sylhet, Bangladesh with a maximum particle size of 4.75 millimeters, was utilized, and as coarse aggregates, crushed stone with a maximum particle size of 12 millimeters was utilized. Table 2 presents the physical properties of these aggregates. Figure 3 illustrates the gradation curves for the fine and coarse aggregates that were obtained using sieve analysis in accordance with ASTM C136 / C136M-19 [32]. To achieve high workability, a Poly Carboxylate Ether-based high-range water-reducing admixture was used, complying ASTM C494/C494M-08 [33]. Fresh distilled water from the laboratory was utilized for mixing.

Table 1. Properties of Cementitious Materials.

Ingredients	OPC	BLA
Calcium Oxide (CaO)	63.34	19.36
Silicon Dioxide (SiO_2)	21.32	43.88
Aluminum Oxide (Al_2O_3)	4.84	5.38
Ferric Oxide (Fe_2O_3)	3.75	4.48
Magnesium Oxide (MgO)	1.85	8.81
Sulfur Trioxide (SO_3)	2.34	1.97
Sodium oxide (Na_2O)	0.18	0.44
Loss of Ignition (LOI)	1.39	5.02
Specific Gravity	3.04	2.63

Table 2. Physical Properties of Aggregates.

Properties	Unit	Fine aggregate	Coarse aggregate
Loose unit weight	Kg/m^3	1412.81	1525.32
Compacted unit weight	Kg/m^3	1594.64	1698.16
Fineness Modulus	-	2.353	6.05
Moisture Content (w)	%	1.3	1.95
Absorption	%	1.62	1.18
Specific gravity (Gs)		2.64	2.72

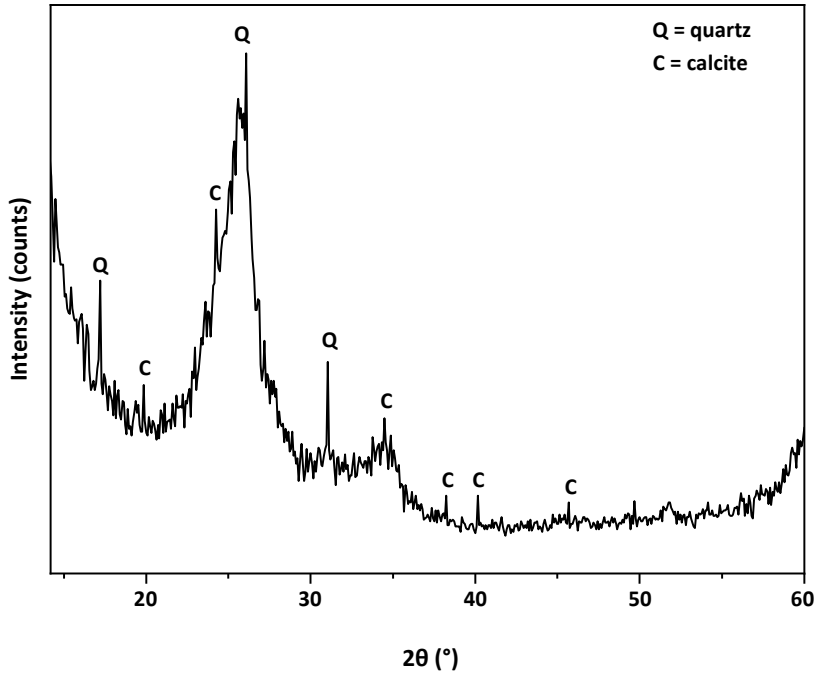

Figure 1. XRD of banana leaf ash

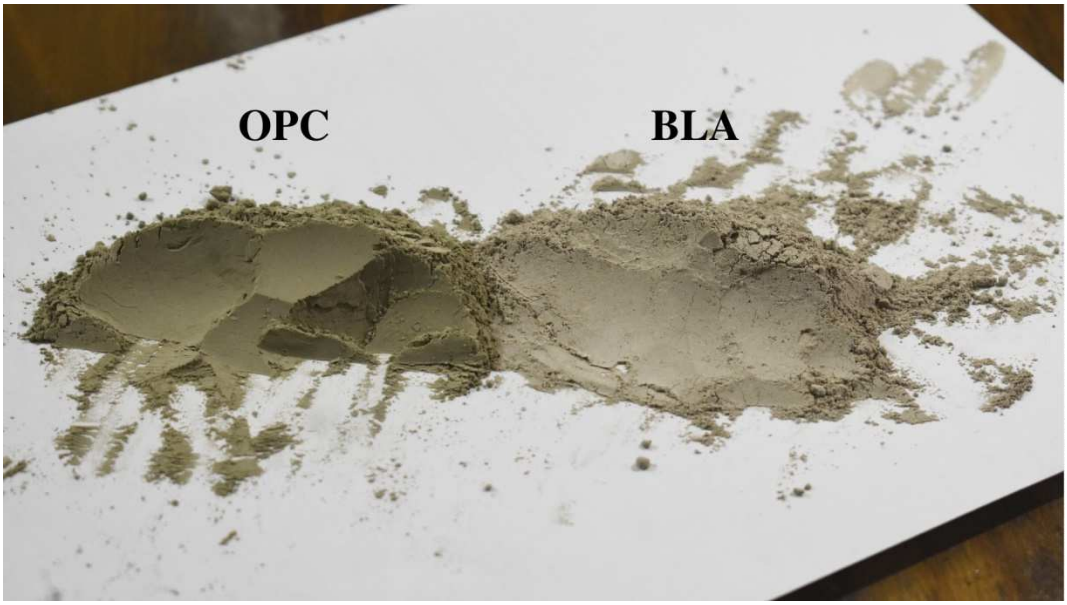

Figure 2. Cementitious Materials used in the experiment OPC and BLA.

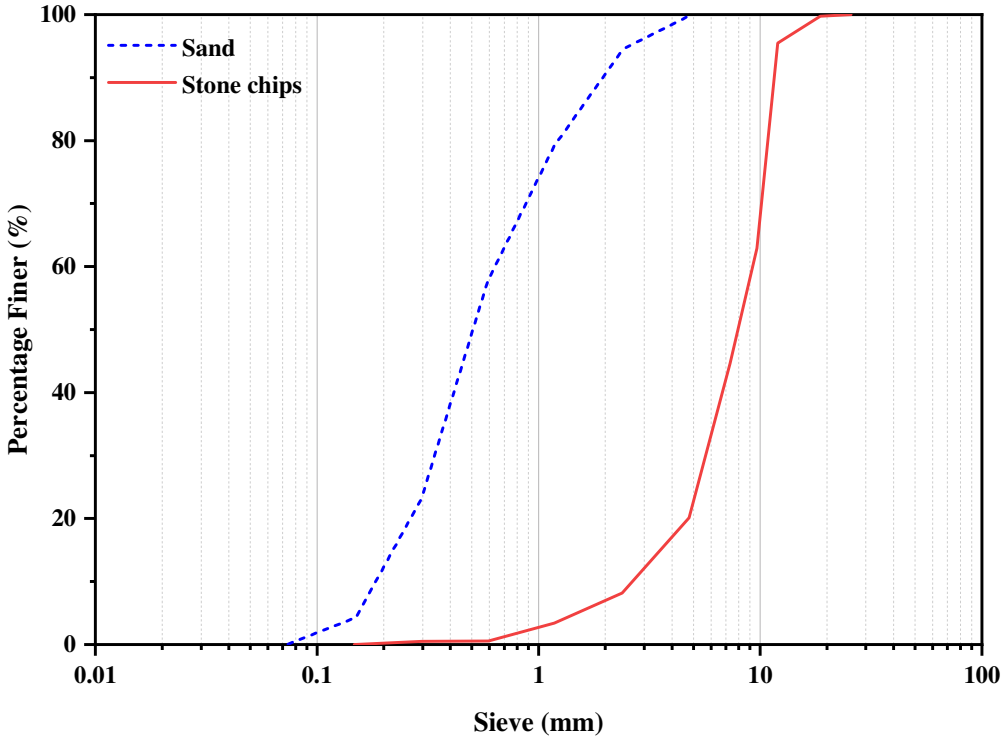

Figure 3. Gradation curve of aggregates (fine and coarse aggregates).

2.2. Mix proportions and specimen preparation

The objective of the control mixture was to achieve a compressive strength of at least 35 MPa at the age of 28 days according to IS 10262 [34]. For slump flow SF2 (slump flow 660-750mm) class was taken, additionally for viscosity V1 class (V funnel flow time ≤ 8s) was considered to design mix ratios. After a comprehensive trial testing, several experimental mixtures were created by varying the water binder ratio and superplasticizer dosages. For all concrete mixtures in this study, a consistent water to binder ratio of 0.29 was preserved. A total of four distinct categories of mix designs were generated by substituting the cement with variable percentages of BLA to evaluate the fresh and hardened properties of the concrete. In the first mix, also known as a control mix (BLA0), the weights of OPC, fine aggregate, and coarse aggregates were maintained at 1:1.75:1.5. The remaining three mixes were produced by substituting 10%, 20%, or 30% of the BLA, and they were designated as the BLA10, BLA20, and BLA30 correspondingly. The proportions of all mixtures are detailed in Table 3.

For mixing all the batches, a roller arm pan type mixing machine with 7.5 HP and a capacity of 100 liters was utilized. The coarse aggregate was first placed into the mixing machine to produce SCC, followed by fine aggregate and binders. The components were then dry-mixed for one minute to ensure consistent distribution. The water and Superplasticizer were then added to the mix and continued for a further 4.5 minutes till visibly flowable. The EFNARC [35] criteria were used to produce all compositions.

Cylindrical specimens of 100 mm in diameter and 200 mm in length, as well as a concrete beam measuring 100 mm in width and 500 mm in length, were created. The samples were stored at room temperature in a sealed plastic container until they had hardened. After 48 hours, the specimens were carefully demolded to avoid damaging the surface. All SCC samples were submerged in fresh water for 7, 14, 28, and 56 curing days.

Table 3. Mix Proportion for the Study.

Mix ID	Cement (kg/m^3)	BLA (kg/m^3)	Sand (kg/m^3)	Stone chips (kg/m^3)	Water (kg/m^3)	Superplasticizer (%)
BLA0	500	0	875	750	168	1.11
BLA10	450	50	875	750	168	1.11

BLA20	400	100	875	750	168	1.11
BLA30	350	150	875	750	168	1.11

2.3. Test methods

The workability parameters of the SCC, including flowability, viscosity, and passing ability, were evaluated in accordance with the European standard for SCC [35]. These trials were carried out within 15 minutes of the concrete being mixed so that the testing could be carried out on concrete when it was still in its fresh state. Slump flow was used in accordance with BS EN 12350-8 [36] to determine the flowability of the fresh mix. To determine the fresh concrete's viscosity, the T_{500} flow time (the amount of time required to achieve a flow diameter of 500 mm) and the V-funnel time (the amount of time required to flow out of the funnel) were obtained. In accordance with BS EN 12350-10 [37] and BS EN 12350-12 [38], the L-box test and the J-ring test were carried out to evaluate the ability to pass through tight entrances and other obstacles together within a given flow path length. Fig. 4 illustrates the operation process of each test.

a) Slump flow test

b) J-ring test

c) L-box test

d) V-funnel test

Figure 4. Processes for the workability property tests.

The compressive test was performed according to ASTM-C39 [39], while the splitting tensile strength and flexural strength test were performed according to ASTM-C496 [40] and ASTM-C78 [41] respectively after 7 and 28 days of curing. For determining the durability properties of the self-compacting concrete incorporating BLA, rapid chloride penetration and water permeability test was conducted according to ASTM-C1202 [42] and ASTM-C642 [43], respectively, after 56 days. For microstructural analysis, the concrete sample was examined through scanning electron microscopy (SEM). Besides, the thermogravimetric analysis (TGA) was conducted through a Mettler Toledo (SDTA-851) to determine a material's thermal stability and its fraction of volatile components by monitoring the weight change that occurs as a sample is heated at a constant rate.

3. Result and discussions

3.1. Effect of BLA on fresh properties

3.1.1. Slump Flow Test

The graphical representation of slump flow (mm) and BLA replacement rate is shown in Figure 5. All the slump diameters for the four distinct mix designs were within the acceptable

range of 550 mm – 750 mm. As the replacement amount of BLA in the mixture increased, the slump flow values progressively decreased. SCC with 0% BLA had a slump flow of 748 mm, indicating high flowability of the control mixture. Mix BLA10, BLA20, and BLA30 with 10%, 20%, and 30% BLA substitution had decreasing slump values of 692mm, 656mm, and 584mm, correspondingly.

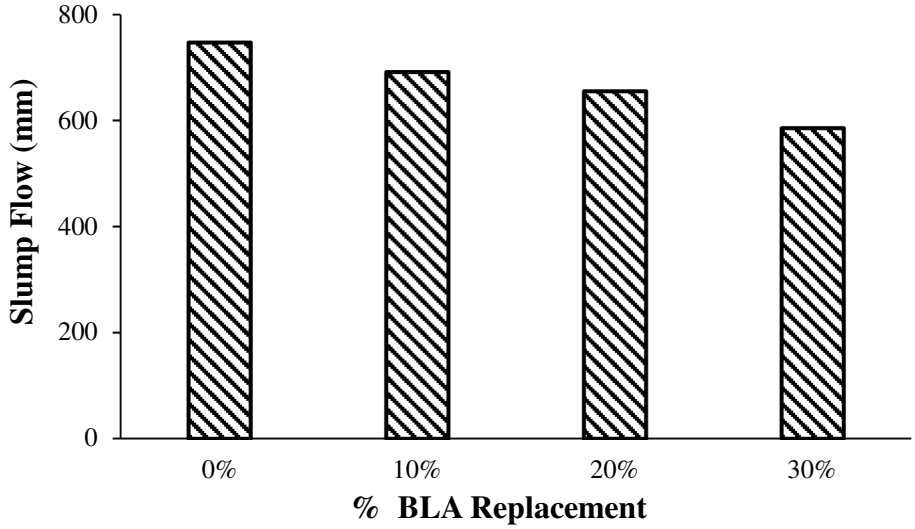

Figure 5. Slump flow of SCC with varying percentage of BLA.

This variation of slump might be due to the BLA's high absorption capacity and rough surface texture. In addition, BLA has greater surface area than cement, which raised water consumption and might cause slump flow values to be lower. These findings are consistent with those of a study that looked at the qualities of self-compacting concrete made using bagasse ash as a partial replacement for cement [44]. Rice husk ash was incorporated by Chopra and Siddique [45] as a cement alternative and observed a similar decrease in flow with an increase in ash concentration. A similar trend is also seen in the study conducted by Tavares et al. [46]. Moreover, the slump flow value of all BLA-containing mixes satisfies the EFNARC (2005) guidelines. As per the EFNARC (2005) standard, all mixes belong to the second class (SF2) and can be used in a variety of applications, such as the castings of columns and walls with a reasonable level of surface polish as well as the building of segregation-resistant structures under specific conditions.

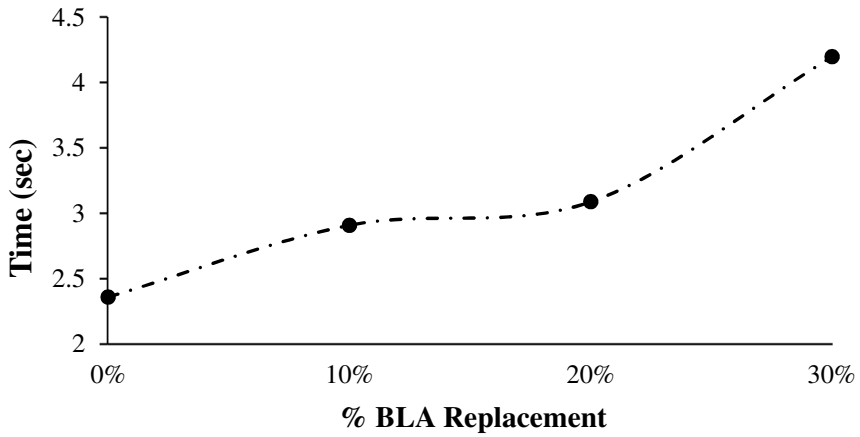

Figure 6. T_{50} of SCC with varying percentage of BLA.

The slump flow tests could also be used to determine the viscosity by calculating the time necessary for attaining a 50-cm flow diameter (T50). The 50-cm flow time, T50 is calculated whenever the SCC reaches the 50-cm circle on the testing plate. From Figure 6, the 2–5 second limit of every measured result confirmed satisfying performance according to EFNARC (2005). The control mix depicted the least time to reach the 50 cm circle, which was 2.36 seconds. But the highest was noticed for the BLA30 mix, around 4.20 seconds. Since BLA has a larger specific surface area, it impacts the flow of concrete mixes, taking longer to reach the 500 mm circle as the percentage of BLA increases.

3.1.2. J-Ring Test

According to Figure 7, the J-ring flow rates decreased as the percentage of BLA increased, despite the fact that the mixtures maintained within the permissible range. The control mixture had a J-ring diameter of 706 mm, indicating excellent passing ability, as well as voids filling capacity. As the passing ability of the mixes declined with the gradual increase of BLA concentration. The lowest J-ring diameter was 553 mm for BLA30 (30% replacement), reducing about 20% of the flow dia. The variation in slump flow between with and without J-ring equipment will not be larger than 50 mm for concrete to ensure the adequate passing ability. According to ASTM-C1621 [47], the flow difference ranges from 33 to 47 mm, indicating a visible to minor blockage evaluation. The higher specific surface area of banana leaf ash particles and the cellur porousness results in substantial water absorption which decreases the passing ability of the SCC.

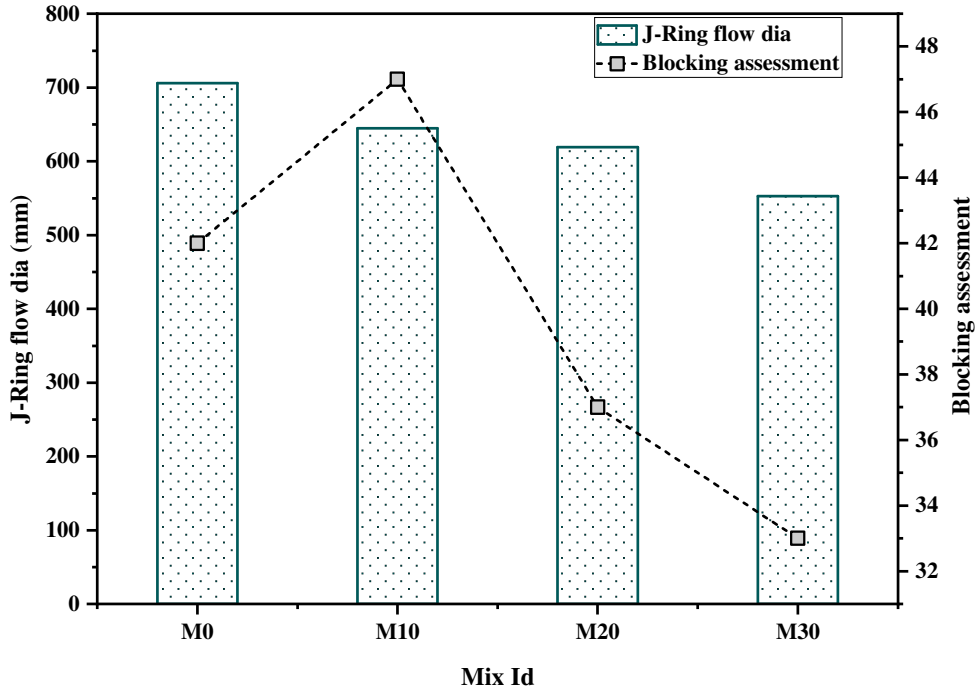

Figure 7. J-Ring slump flow and blocking index of SCC with varying concentrations of BLA.

3.1.3. L-Box Test

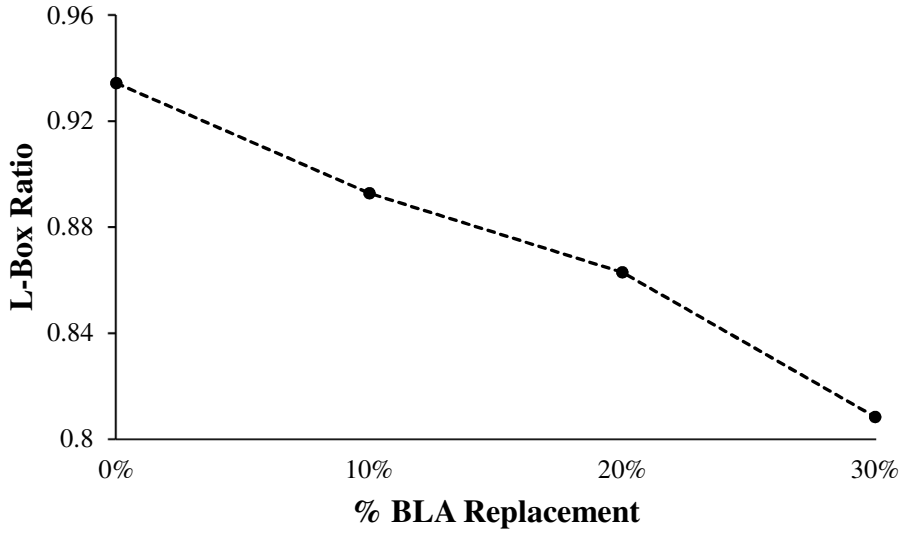

Figure 8. L-Box blocking ratio of SCC with varying percentage of BLA.

The findings of the L-box test, which are depicted in Figure 8, indicate that the ratio of L-box dropped as the amount of BLA substitution increased. The experimental readings achieved in the L-box test were varied from 0.81 to 0.93. The ratio H2/H1 was maximum for control mix (BLA0) which is 0.93 while for BLA10 (10%), BLA20 (20%) and BLA30 (30%) the values were 0.89, 0.86 and 0.81 respectively.

The decremental pattern of the L-box ratio can be explained by the fact that BLA's specific surface absorption capacity are greater than that of OPC. According to the EFNARC guideline, the blocking ratio has to be between 0.8 and 1.0, and all of the produced fresh SCC mixes met the requirements. As a result, all the mixes met the fresh behavior standards for concreate's passing ability. According to the findings, all combinations have sufficient passage capacity, therefore, may be employed in situations requiring circulation across clogged reinforcement.

3.1.4. V-Funnel Test

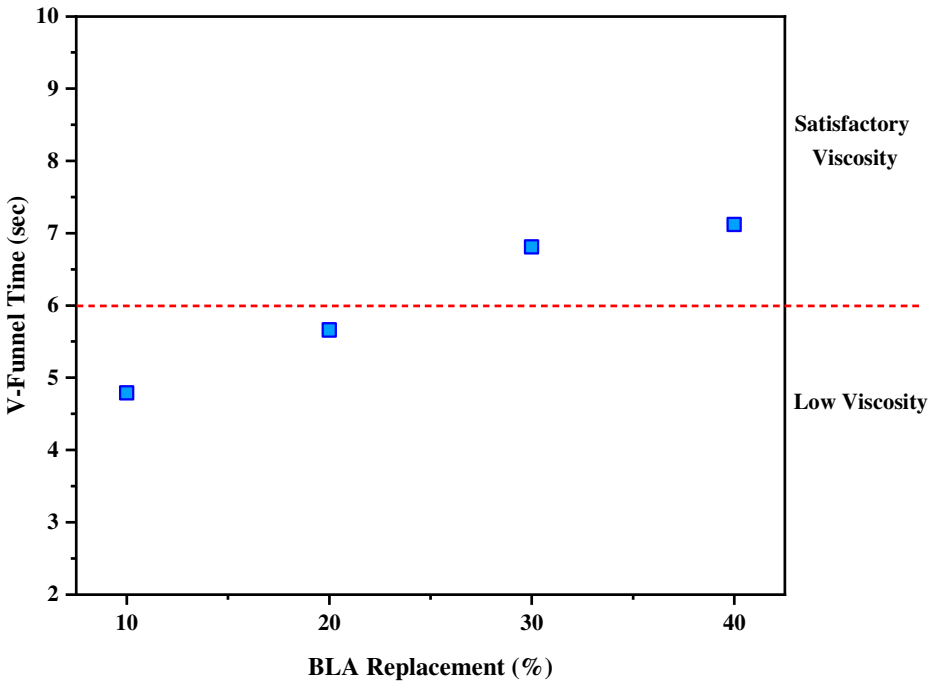

Figure 9. V-funnel flow time of SCC with varying percentage of BLA.

The V-funnel test determines the capacity to pass through a tight hole while also indicating concrete segregation. As per EFNARC [35], SCC's permissible V-Funnel flow time is between 6 and 12 seconds. Figure 9 depicts the outcome of the V-Funnel test. Although a shorter V-funnel time indicates the filling capacity of a mixture, it also indicates lesser viscosity. Akram et al. [44] concluded that the V funnel measured values for SCC mixes in most cases remain lower than six seconds, which is more crucial for filling ability.

As shown in figure 9, the V-funnel flow time of SCC mixtures raised with the increase of BLA percentage. Among the four mix designs, the flow times of the BLA0, BLA10 were less than the minimum EFNARC recommended value (i.e. 6 s), demonstrating the low viscosity of the concrete with BLA inclusion levels up to 10%. However, the BLA30 (30% BLA) had the longest V-funnel time with satisfactory viscosity. This might be due to the lower density of BLA compared to the Portland cement. As a result, the incorporation of BLA raised the volume of the paste as well as the viscosity of the fresh SCC mixes.

3.2. Effect of BLA on hardened properties

3.2.1. Compressive Strength Test

Table 4 summarizes the compressive strength test findings with mean strength, co-efficient of variation, standard deviation, standard error as well as lower, upper bound of 95% confidence interval. The findings demonstrate that the compressive strength is gradually deteriorating with the amount of BLA used as a cement substitute increases. The strength varied from 35.12 MPa to 25.96 MPa and 39.10 MPa to 31.35 MPa for 7 and 28 days respectively. For 7 days, the standard deviation ranged between 1.406 to 0.235, with the standards error about 0.812 to 0.136 and the coefficient of variation about 4% to 0.9%. For 7 days, the standard deviation ranged between 0.508 to 0.138, with the standards error about 0.293 to 0.080 and the coefficient of variation about 1.5% to 0.4%.

Table 4. Compressive Strength Test Result Data of All SCC Mixes.

Mix ID	Strength (MPa)	Mean strength (MPa)	Standard deviation SD	Co-efficient of	Standard Error SE	95% Confidence interval

	Days	C1	C2	C3			variation CV		Upper Limit	Lower Limit
BLA0	7	35.17	33.69	36.5	35.12	1.406	0.04	0.812	38.612	31.628
	28	38.97	39.61	38.72	39.1	0.459	0.012	0.265	40.24	37.96
BLA10	7	32.56	32.29	31.54	32.13	0.528	0.016	0.305	33.443	30.817
	28	37.15	36.94	36.89	36.99	0.138	0.004	0.08	37.336	36.651
BLA20	7	31.91	31.77	31.25	31.64	0.348	0.011	0.201	32.507	30.779
	28	34.88	35.48	34.47	34.94	0.508	0.015	0.293	36.205	33.681
BLA30	7	25.97	26.19	25.72	25.96	0.235	0.009	0.136	26.544	25.376
	28	31.46	30.99	31.61	31.35	0.323	0.01	0.187	32.157	30.55

The compressive strength of all SCC mixtures is represented in Figure 10. For 7 days, the lowest flexural strength observed in BLA30 mix (30% BLA replacement) about 25.96 MPa with 95% confidence intervals about 25.376 MPa to 26.544 MPa, and, the BLA0 (control mix) exhibited the maximum strength around 35.12 MPa with 95% confidence intervals about 31.638 MPa to 38.612 MPa. Furthermore, for 28 days, the lowest flexural strength observed in BLA30 mix (30% BLA replacement) about 31.35 MPa with 95 % confidence intervals about 32.157 MPa to 32.157 MPa and the BLA0 (control mix) exhibited the maximum strength around 39.10 MPa with 95 % confidence intervals about 40.240 MPa to 37.960 MPa. The principal binding ingredient, cement was substituted with a slower-reacting material, BLA which resulted in the drop in strength.

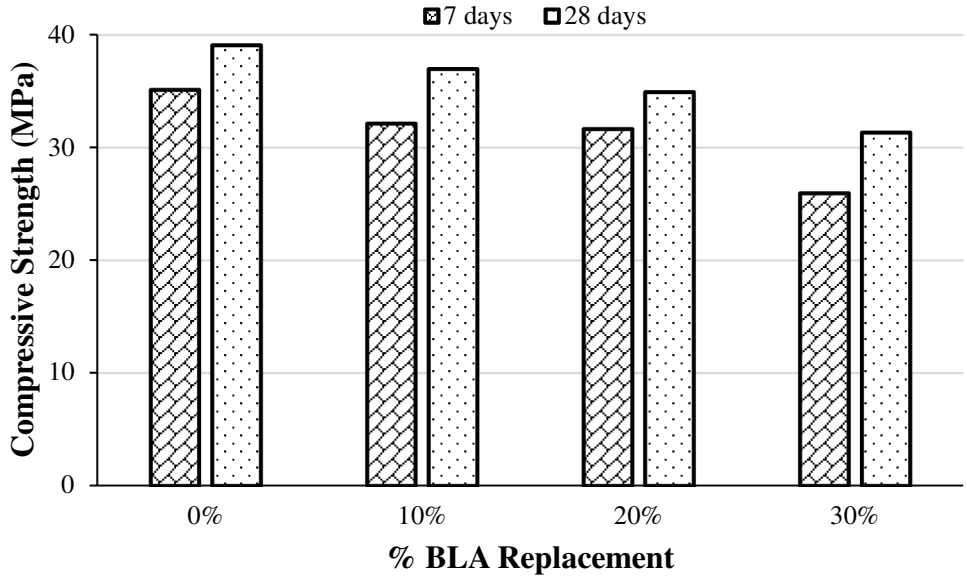

Figure 10. Compressive strength test results of all SCC mixes at 7 and 28 days.

Figure 11 shows the variation of compressive strength with varying concentration of BLA than the control mixture. After 7 and 28 days, the strength reduction around 26.08% and 19.81% for concrete mix with 30% BLA. Concrete mixes containing 10% and 20% BLA had compressive strengths of 32.13 MPa and 31.64 MPa which is 8.51% and 9.91% lower after 7 days, whereas for 28 days, it was 36.99 MPa and 34.94 MPa that is 5.39% and 10.63% lower than the control mix.

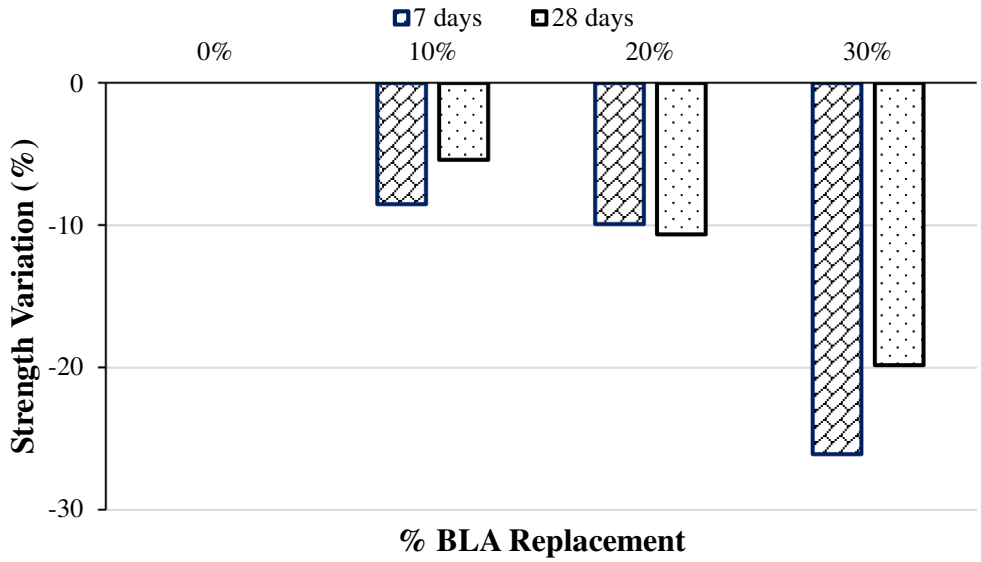

Figure 11. Variations of compressive strength of SCC mixes at 7 and 28 days.

This observation is consistent with the findings of other research studies with varying BLA concentrations [48-50]. Slight strength differences have been reported up to 20% cement substitution with BLA mix compared to control mix, but subsequently the difference rapidly disappears. The explanation for this is because while cement provides sufficient binding capacity for 100% cement mortar and concrete mixes, there will still be some porous gaps or voids in the mortar or concrete mass. When BLA is used to replace cement up to 20%, such empty areas are filled with both BLA and absorbed water, since BLA has a higher capacity to absorb water than cement. As a result, the binding strengths and void-free state of the mortar and concrete masses are successfully achieved, resulting in a strong compressive strength.

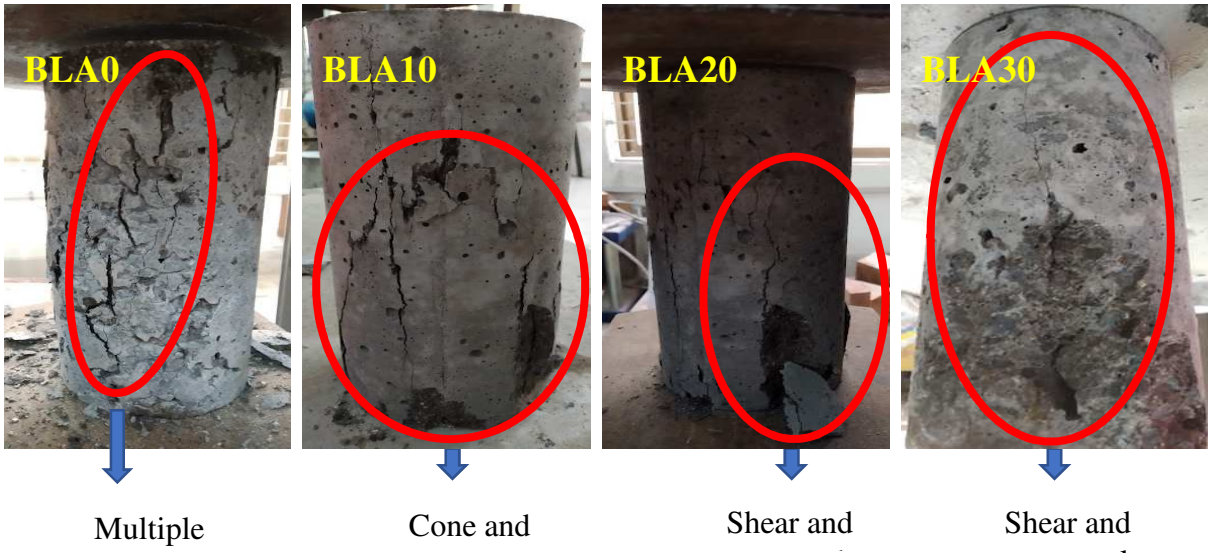

Figure 12. Different failure pattern of cylindrical concrete specimens incorporating different percentage of BLA.

During compressive strength testing, the cylinder was explored in depth and the failure modes were noted. For cylindrical specimens, six different failure modes can emerge as per (ASTM-C39 [39]. Cone, columnar and shear cracks are identified as mostly occurred cracks. The BLA20 and BLA30 specimens both feature a well-formed cone on one end that is a shear crack as well as the vertical cracks going throughout the caps, and no well-defined cracks on the other end (Type 2), as shown in Figure 12. Multiple distinct columnar cracks go through both endpoints in concrete samples of mix BLA0, with no well-defined cones (type 3). These are the most evident and frequent modes of failure. Types 4, 5, and 6 imply an issue with concreting and specimen preparations.

3.2.2. Compressive Strength Test of Mortar Specimens

Table 5 summarizes the compressive strength test findings with mean strength, co-efficient of variation, standard deviation, standard error as well as lower, upper bound of 95% confidence interval. The findings demonstrate that the compressive strength is gradually deteriorating. The strength varied from 17.75 MPa to 13.64 MPa and 24.24 MPa to 19.59 MPa for 7 and 28 days respectively. For 7 days, the standard deviation ranged between 0.565 to 0.076 with the standards error about 0.326 to 0.044 and the coefficient of variation about 3.9% to 0.5%. On the other hand, for 28 days, the standard deviation ranged between 0.489 to 0.153 with the standards error about 0.282 to 0.088 and the coefficient of variation about 2.5% to 0.7%.

Table 5. Compressive strength test result data of mortar

Mix ID	Strength (MPa)				Mean strength (MPa)	Standard deviation SD	Co-efficient of variation CV	Standard Error SE	95% Confidence interval	
	Days	C1	C2	C3					Upper Limit	Lower Limit
BLA0	7	17.57	17.98	17.69	17.75	0.211	0.012	0.122	18.27	17.223
	28	24.53	24.17	24.01	24.24	0.266	0.011	0.154	24.898	23.575
BLA10	7	16.03	15.89	15.91	15.94	0.076	0.005	0.044	16.131	15.755
	28	22.67	22.23	22.62	22.51	0.241	0.011	0.139	23.105	21.908
BLA20	7	15.11	14.09	14.18	14.46	0.565	0.039	0.326	15.863	13.057
	28	20.95	21.18	20.89	21.01	0.153	0.007	0.088	21.387	20.626
BLA30	7	13.27	13.91	13.75	13.64	0.333	0.024	0.192	14.471	12.816
	28	19.52	19.14	20.11	19.59	0.489	0.025	0.282	20.804	18.376

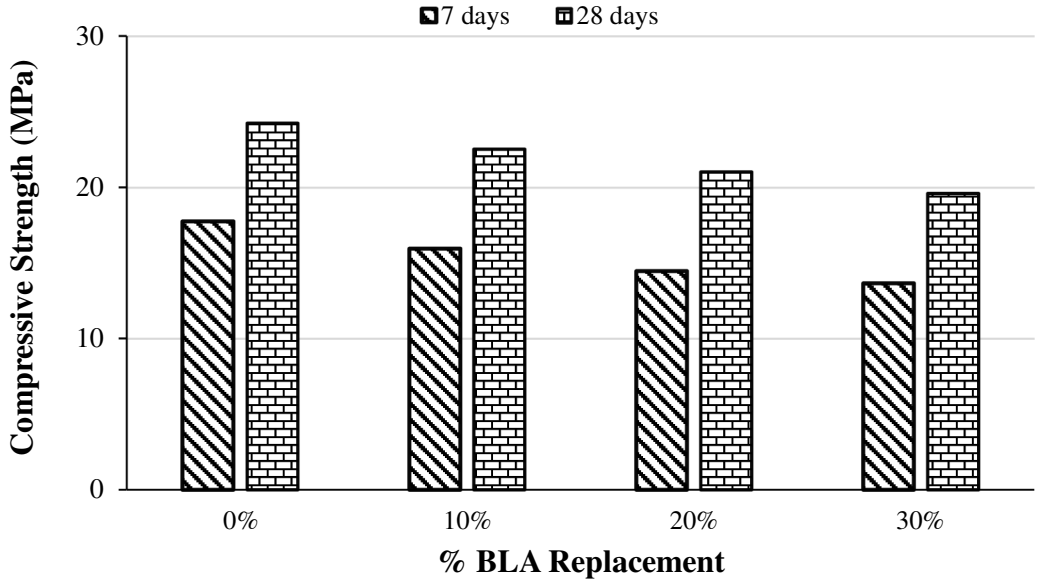

Figure 13. Compressive strength test results of all mortar at 7 and 28 days.

The compressive strength of mortar is represented in Figure 13. The compressive strength of control mix (BLA0) is 17.75 MPa which is maximum at 7 days and the minimum compressive strength is 13.64 MPa of BLA30 mix. The compressive strength of other two mix ID, BLA10 and BLA20 is 15.94 MPa and 14.46 MPa respectively. The maximum and minimum compressive strength is 24.24 MPa and 19.59 MPa of BLA0 and BLA30 specimen respectively at 28 days.

Figure14 shows the variation of compressive strength with varying concentration of BLA than the control mixture. After 7 and 28 days, the strength reduction around 23.12% and 19.17% for concrete mix with 30% BLA. Concrete mixes containing 10% and 20% BLA had compressive strengths of 15.94 MPa and 14.46 MPa, respectively, which were 10.16% and 18.52% lower than the control mix after 7 days, whereas for 28 days, it was 22.51 MPa and 21.01 MPa that is 7.14% and 13.33% lower than the control mix.

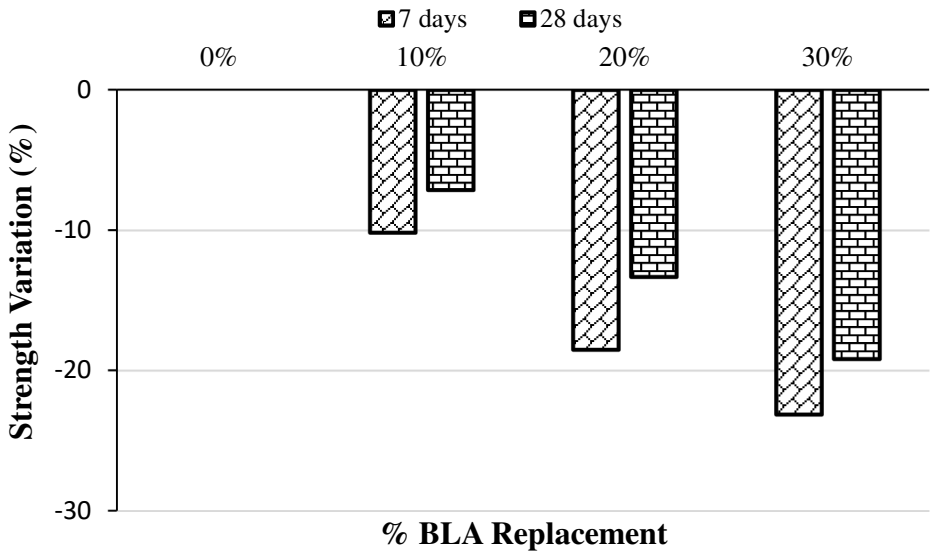

Figure 14. Variations of compressive strength of all mortar at 7 and 28 days.

The compressive strength variations after 28 days are lower than compressive strength variations after 7 days for all samples of any percent replacement. It indicates that, if cement is replaced by BLA partially, compressive strengths are improved if more curing is done. The reason behind that could be the BLA mixed concrete absorb water nicely and fills the porous spaces among the concrete mass. Hence the compressive strength is improved for much curing.

Figure 15. Different failure pattern of cube specimens incorporating different percentage of BLA.

Figure 15 shows the many failure mechanisms that happened during the experiment. Non-explosive failure was assigned to it. In accordance with ASTM-C109 [51], such a trend of failure satisfied the failure modes. Visual examination additionally revealed that the breaking in the majority of the cube samples was at a 45° angle to the axis near the edges.

3.2.3. Splitting Tensile Strength Test

Table 6 summarizes the split tensile strength test findings with mean strength, co-efficient of variation, standard deviation, standard error as well as lower, upper bound of 95% confidence interval. The splitting tensile strength varied from 2.713 MPa to 4.190 MPa and 3.12 MPa to 4.76 MPa for 7 and 28 days respectively. For 7 days, the standard deviation ranged between 0.090 to 0.197 with the standards error about 0.052 to 0.114 and the coefficient of variation about 2.8% to 4.7%. On the other hand, for 28 days, the standard deviation varied between 0.255 to 0.070 with the standards error about 0.147 to 0.041 and the coefficient of variation about 5.4% to 1.9%.

Table 6. Splitting Tensile Strength Test Result Data of All SCC Mixes.

Mix ID	Strength (MPa)			Mean strength (MPa)	Standard deviation SD	Co-efficient of variation CV	Standard Error SE	95% Confidence interval	
	Days	C1	C2	C3				Upper Limit	Lower Limit
BLA0	7	3.97	4.25	4.35	4.19	0.197	0.047	0.114	4.679	3.701
	28	5.02	4.51	4.76	4.76	0.255	0.054	0.147	5.397	4.129
BLA10	7	3.68	3.61	3.39	3.56	0.151	0.043	0.087	3.936	3.184
	28	3.99	4.16	4.27	4.14	0.141	0.034	0.081	4.49	3.789
BLA20	7	3.17	3.35	3.25	3.26	0.09	0.028	0.052	3.481	3.033
	28	3.65	3.79	3.71	3.72	0.07	0.019	0.041	3.891	3.542
BLA30	7	2.74	2.59	2.81	2.71	0.112	0.041	0.065	2.993	2.434
	28	2.98	3.16	3.21	3.12	0.121	0.039	0.069	3.417	2.816

The splitting tensile strength of all SCC mixtures is represented in Figure 16. At 7 and 28 days, the tensile strength of control mixture BLA0 was 4.19 MPa and 4.76 MPa, respectively. The results specified that adding BLA into concrete decreased its flexural strength compared to the control mix. For 7 days, the lowest flexural strength observed in BLA30 mix (30% BLA replacement) about 2.713 MPa with 95% confidence intervals of 2.434 MPa and 2.993 MPa; and, the BLA0 (control mix) exhibited the maximum strength around 4.190 MPa with 95% confidence intervals of 4.679 MPa and 3.701 MPa. On the other hand, the lowest flexural strength observed in BLA30 mix (30% BLA replacement) about 3.12 MPa with 95% confidence intervals of 2.816 MPa and 3.417 MPa; and, the BLA0 (control mix) exhibited the maximum strength around 4.76 MPa with 95% confidence intervals of 4.129 MPa and 5.397 MPa.

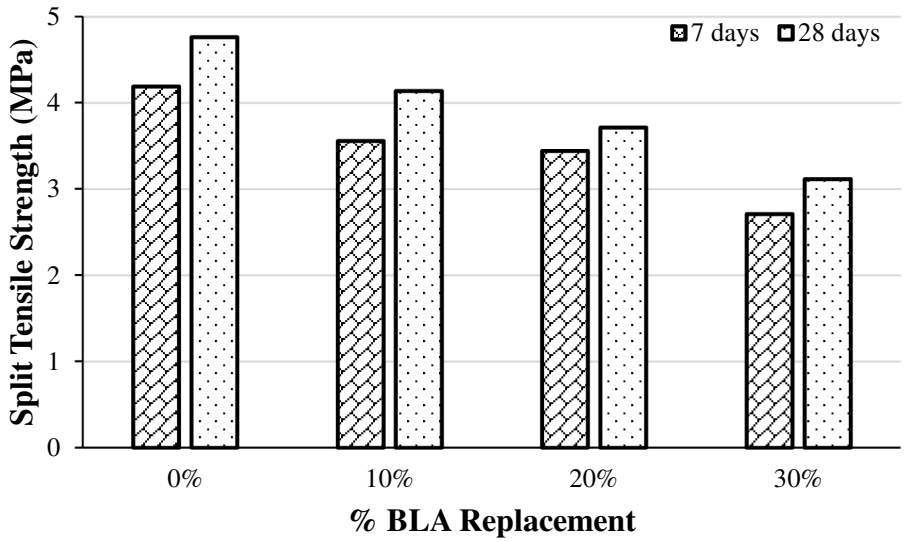

Figure 16. Split tensile strength test results of all SCC mixes at 7 days.

Figure 17 shows the variation of split tensile strength with varying concentration of BLA than the control mixture. After 7 and 28 days, the strength reduction around 15.04%, 17.8% and 13.09%, 21.97% were noticed in concrete mix with 10% and 20% BLA concentration, respectively. The maximum percent of strength change was found 35.25% and 34.57% for concrete mix with 30% BLA after 7 and 28 days respectively.

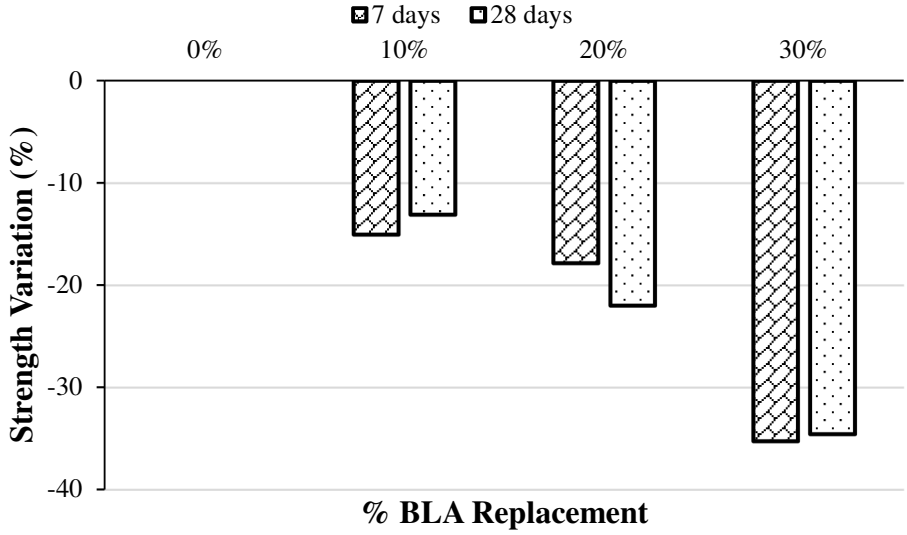

Figure 17. Variations of split tensile strength of SCC mixes at 7 days.

The acceptable split tensile strength is approximately around 2-5 MPa as per ACI-318 [52]. In this study, the split tensile strength of all SCC mixes is within the acceptable range. The result has shown a tendency of decrease with the replacement of BLA percentage. But the strength of mix BLA20 with 20% BLA incorporation was found to be almost similar to control concrete strength. The failure pattern of mixes is illustrated in Figure 18. Most of the cracks observed along the failure plane. Both the principle and secondary crack are observed.

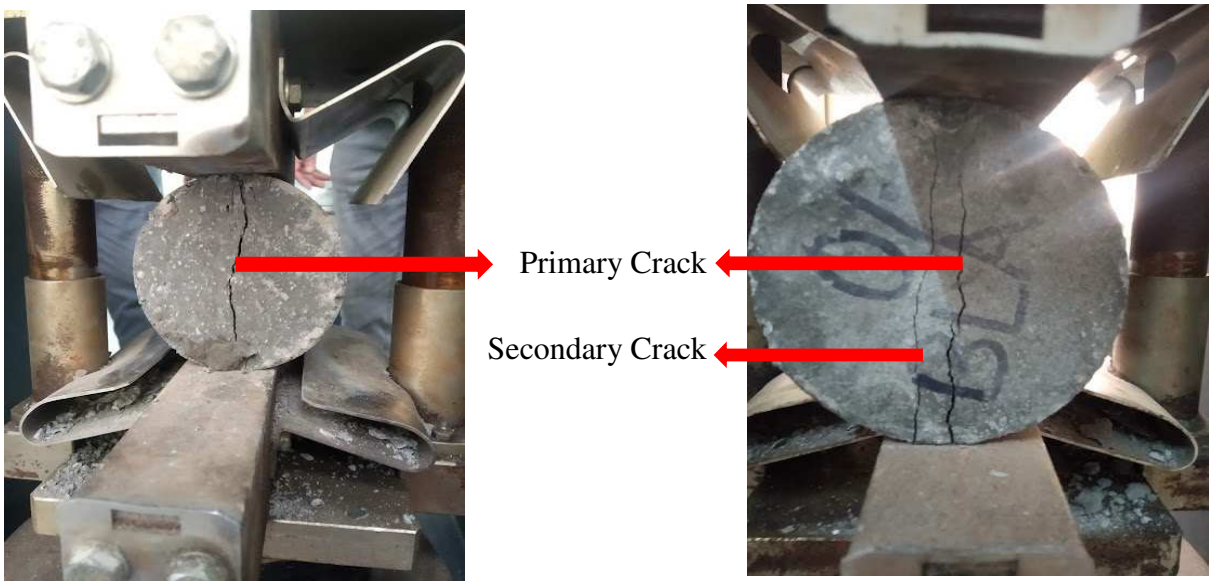

Figure 18. Different failure patterns of cylindrical concrete specimens incorporating different percentages of BLA.

3.2.4. Flexure Strength Test

Table 7 summarizes the flexural strength test findings with mean strength, coefficient of variation, standard deviation, standard error, as well as lower and upper bound of 95% confidence interval. Flexure strength varied from 6.663 MPa to 5.043 MPa and 7.95 MPa to 5.92 MPa for 7 and 28 days, respectively. For 7 days, the standard deviation ranged between 0.074 and 0.140 with the standards error about 0.043 to 0.081 and the coefficient of variation about 1.2% to 2.4%. On the other hand, for 28 days, the standard deviation varied between 0.107 and 0.055 with the standards error about 0.062 to 0.032 and the coefficient of variation about 1.6% to 0.8%.

Table 7. Flexural Strength Test Result Data of All SCC Mixes.

Mix ID	Strength (MPa)				Mean strength (MPa)	Standard deviation SD	Co-efficient of variation CV	Standard Error SE	95% Confidence interval	
	Days	C1	C2	C3					Upper Limit	Lower Limit
BLA0	7	6.79	6.54	6.66	6.66	0.125	0.019	0.072	6.974	6.353
	28	7.89	8.02	7.95	7.95	0.065	0.008	0.038	8.115	7.792
BLA10	7	6.27	6.12	6.2	6.2	0.075	0.012	0.043	6.383	6.01
	28	7.17	7.06	7.12	7.12	0.055	0.008	0.032	7.253	6.98
BLA20	7	5.84	5.99	5.71	5.85	0.14	0.024	0.081	6.195	5.499
	28	6.79	6.65	6.58	6.72	0.107	0.016	0.062	6.939	6.408
BLA30	7	4.96	5.1	5.07	5.04	0.074	0.015	0.043	5.226	4.86
	28	5.92	6.01	5.84	5.92	0.085	0.014	0.049	6.135	5.712

The flexure strength of all SCC mixtures is represented in Figure 19. At 7 and 28 days, the flexural strength of control mixture BLA0 was 6.663 MPa and 7.95 MPa, respectively. The results specified that adding BLA into concrete decreased its flexural strength compared to the control mix. For seven days, the lowest flexural strength observed in BLA30 mix (30% BLA replacement) was about 5.043 MPa with 95% confidence intervals of 4.860 MPa and 5.226 MPa; and the BLA0 (control mix) exhibited a maximum strength of around 6.663 MPa with 95% confidence intervals of 6.353 MPa and 6.974 MPa. Moreover, for 28 days, the lowest flexural strength observed in the BLA30 mix (30% BLA replacement) was about 5.92 MPa with 95% confidence intervals of 5.712 MPa and 6.135 MPa; and the BLA0 (control mix) exhibited the maximum strength around 7.95 MPa with 95% confidence interval of 7.792 MPa and 8.115 MPa.

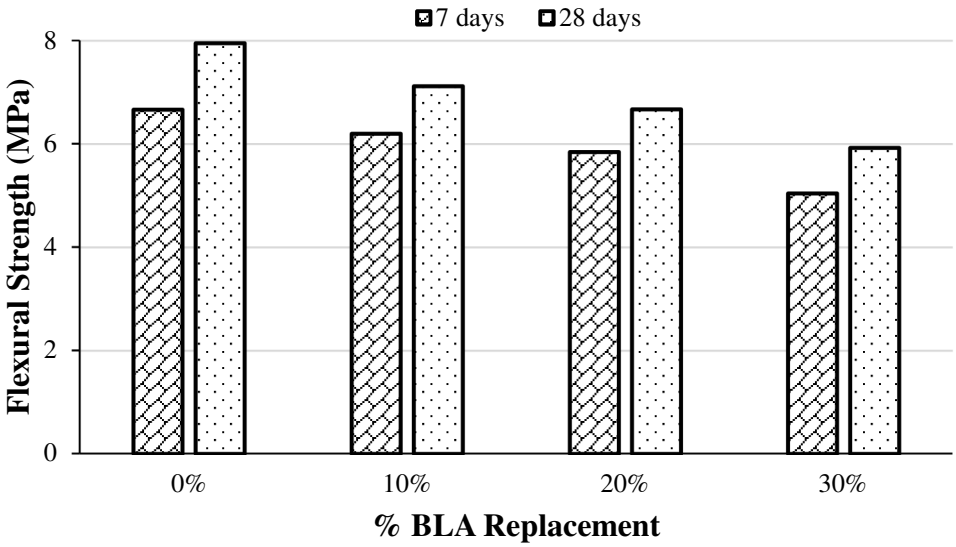

Figure 19. Flexural strength test results of all SCC mixes at 7 days.

Figure 20 shows how the percentage of flexural strength fluctuates as the proportion of BLA differs from the control mixture. After 7 and 28 days, concrete mixes with 10% and 20% BLA concentrations showed a strength drop of roughly 7.00%, 12.25%, and 10.52%, 16.09%, correspondingly. For 7 and 28 days, the most significant percent strength variation was observed to be 24.31% and 25.52% for concrete mixes with 30 percent BLA.

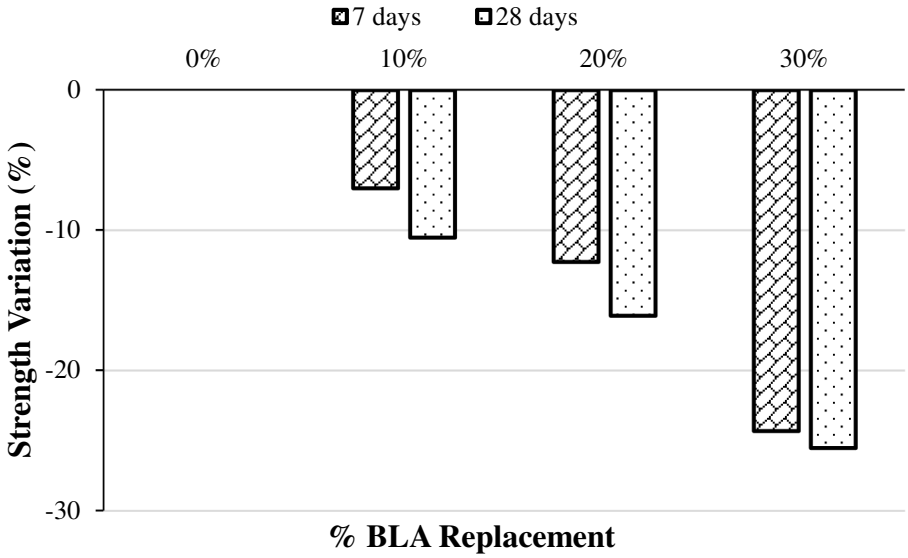

Figure 20. Variations of flexural strength of SCC mixes at 7 days.

The flexural strength test failure pattern of mixes is illustrated in Figure 21. The main characteristics of this crack are that the crack originated in the maximum moment region. It is a single crack, and the maximum width is at the bottom of the beam.

Figure 21. Failure pattern of concrete beam specimens incorporating different % of BLA.

3.2.5. Correlation between Compressive Strength and Split Tensile Strength

Figure 22 shows SCC mixtures' compressive and splitting tensile strength correlation after 7 and 28 days. The mathematical correlation may be utilized for anticipating the hardened properties of concrete by relying on the distinct data. The prediction may be used in finite element analysis to simulate critical components without having to test new materials in different ratios. This might lead to the creation of novel materials as well as mix proportions without the need for expensive costs, extended production time, or bulky equipment. The relationship between compressive and splitting tensile strength for SCC mixtures at 7 and 28 days may be represented by the following two equations (1) and (2), where f_{sp} is the splitting tensile strength and f_c is compressive strength.

$$f_{sp}(7) = 0.1563 f_c - 1.402 \quad \ldots\ldots\ldots\ldots\ldots\ldots\ldots\ldots\ldots\ldots\ldots\ldots \quad (1)$$

$$f_{sp}(28) = 0.2083f_c - 3.4818 \ \ldots\ldots\ldots\ldots\ldots\ldots\ldots\ldots\ldots\ldots\ldots\ldots \quad (2)$$

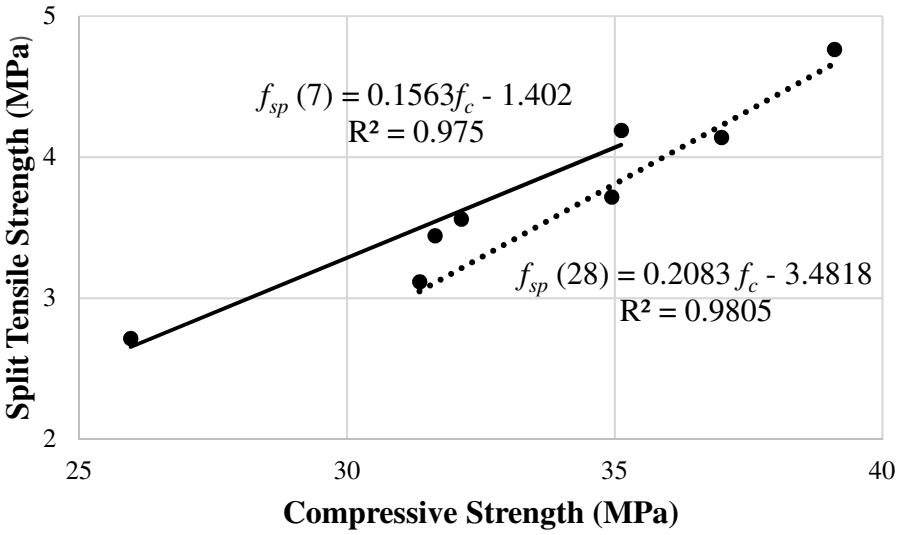

Figure 22. Correlation between compressive strength and splitting tensile strength.

3.2.6. Compressive Strength vs Flexural Strength

The relationship among compressive and flexural strength readings is shown in Figure 23. It demonstrates a positive linear correlation having the high determination coefficients $R^2 = 0.9718$ and 0.9729.

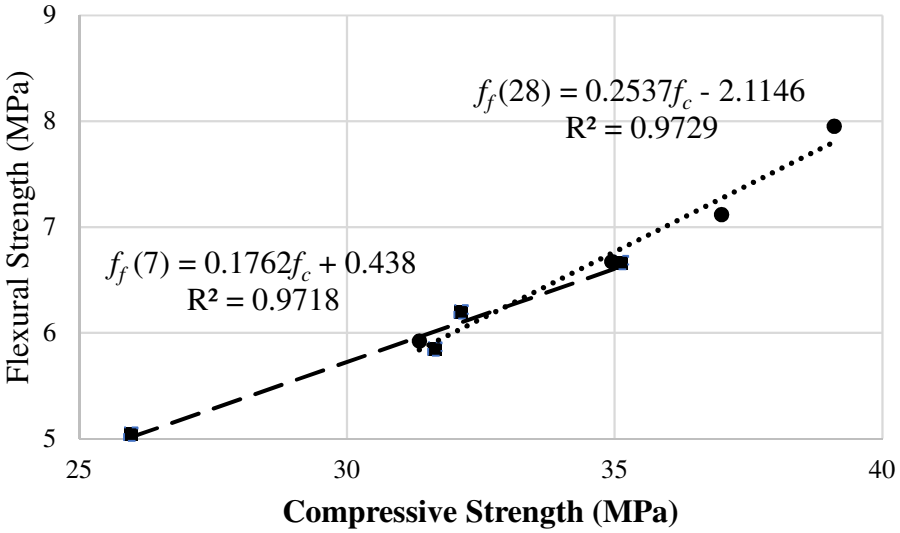

Figure 23. Correlation between compressive strength and flexural strength.

The connection between compressive and flexural strength at 7 and 28 days may be represented by the following two equations, where f_f is the flexural strength and f_c is compressive strength.

$$f_f(7) = 0.1762f_c + 0.438 \quad \ldots\ldots\ldots\ldots\ldots\ldots\ldots\ldots\ldots\ldots\ldots\ldots \quad (3)$$

$$f_f(28) = 0.2573f_c - 2.1146 \quad \ldots\ldots\ldots\ldots\ldots\ldots\ldots\ldots\ldots\ldots\ldots\ldots \quad (4)$$

3.3. Effect of BLA on durability properties of concrete

3.3.1. Rapid Chloride Penetration Test

Rapid Chloride Penetration Test (RCPT) is often used to determine the resistance of specimens to the intrusion of chloride ions into the concrete. The concrete grade can be determined by analyzing the number of charges passed. According to ASTM-C1202 [53] standards, the grade of concrete is represented in Table 8.

Table 8. Rating of Chloride Permeability of Concrete.

Charge Passed (Coulombs)	Chloride Ion penetrability
>4000	High
2000-4000	Moderate
1000-2000	Low
100-1000	Very Low
<100	Negligible

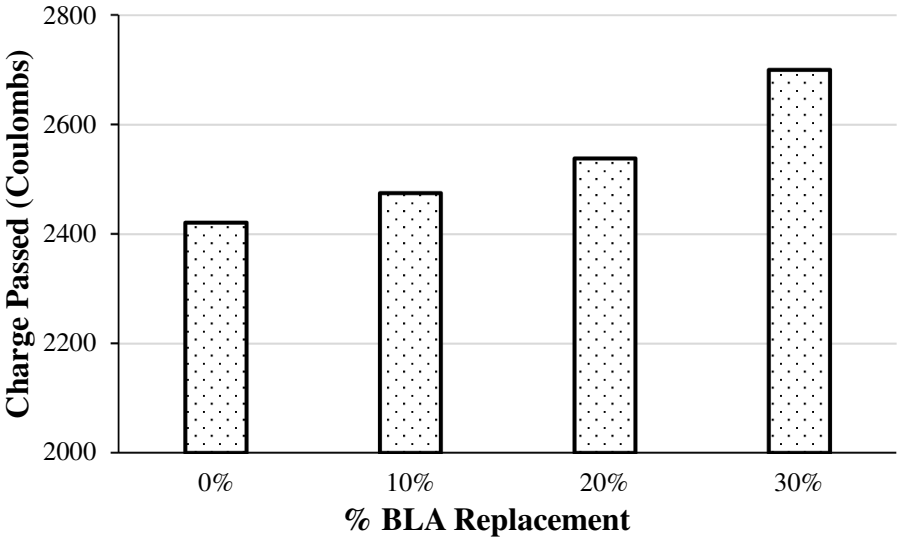

Figure 24. Rapid Chloride Penetration Test results of SCC mixes incorporating different % of BLA.

Figure 24 presents the actual charge transmitted by chloride penetration for all SCC. After 28 days curing, the results were about between 2400 and 2700 coulombs. The findings revealed that 2421 coulombs of charge passed through the BLA0 mixture, which was less than the other mixtures, indicating that the control mixture was more durable. On the other hand, the BLA10, BLA20 and BLA30 mix depicted 2475, 2538, and 2700 coulombs of chloride ion penetration. With the higher concentration of BLA, there was a noticeable rise in the overall chloride penetration. After 28 days of curing, it climbed up 2.23% for BLA10, 4.83% for BLA20, and 11.52% for the BLA30 mix. For mix BLA10, and BLA20, the charge passing is almost identical to the control mix. BLA's pozzolanic interaction with $Ca(OH)_2$ may account for the constrained chloride penetration. Furthermore, the very small dimension of BLA particles aids in the irregularity of the porous system, reducing chloride penetration even further.

3.3.2. Water Permeability Test

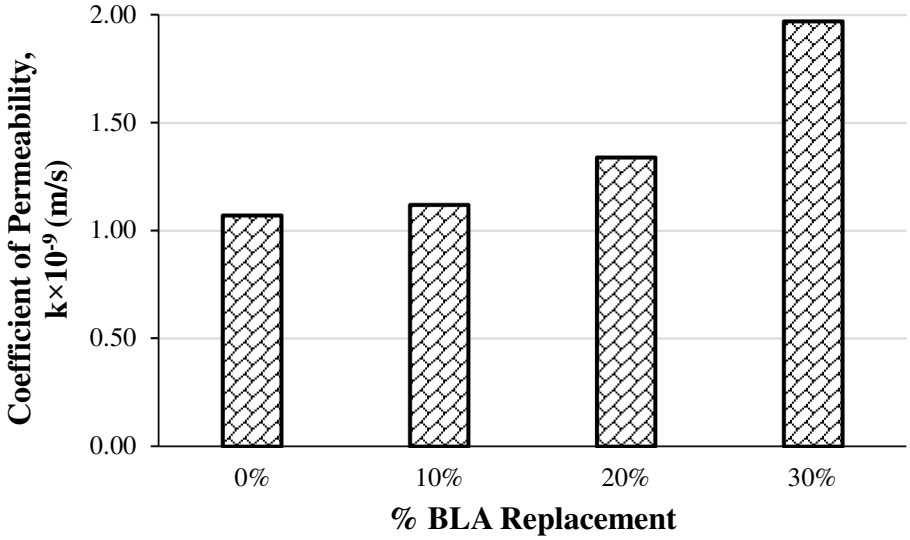

Figure 25. Water permeability test results of SCC mixes incorporating different % of BLA.

Figure 25 shows the permeability coefficient of SCC mixes incorporating a different percentage of BLA. The higher permeability rate reflects the excessive water penetration into the concrete matrix. According to the findings, the water permeability slightly increased with the increasing concentration of BLA. BLA0 had the lowest permeability coefficient of 1.07 × 10^{-9} m/s, whereas BLA30 depicted the highest permeability coefficient of 1.97 x 10^{-9} m/s. In comparison to the control mix (BLA0), the water permeability for mixes containing 10%, and 20% BLA was slightly higher. Such alteration could be attributed to pozzolanic activity as well as an accelerated hydration rate. These results appear to be in line with the findings of past investigations [45, 54]. However, at higher levels of BLA substitution, there was an insufficient quantity of calcium hydroxide to react with the excess BLA, thus creating pores in the mixture and thereby increasing the water absorption.

3.4. Thermogravimetric analysis

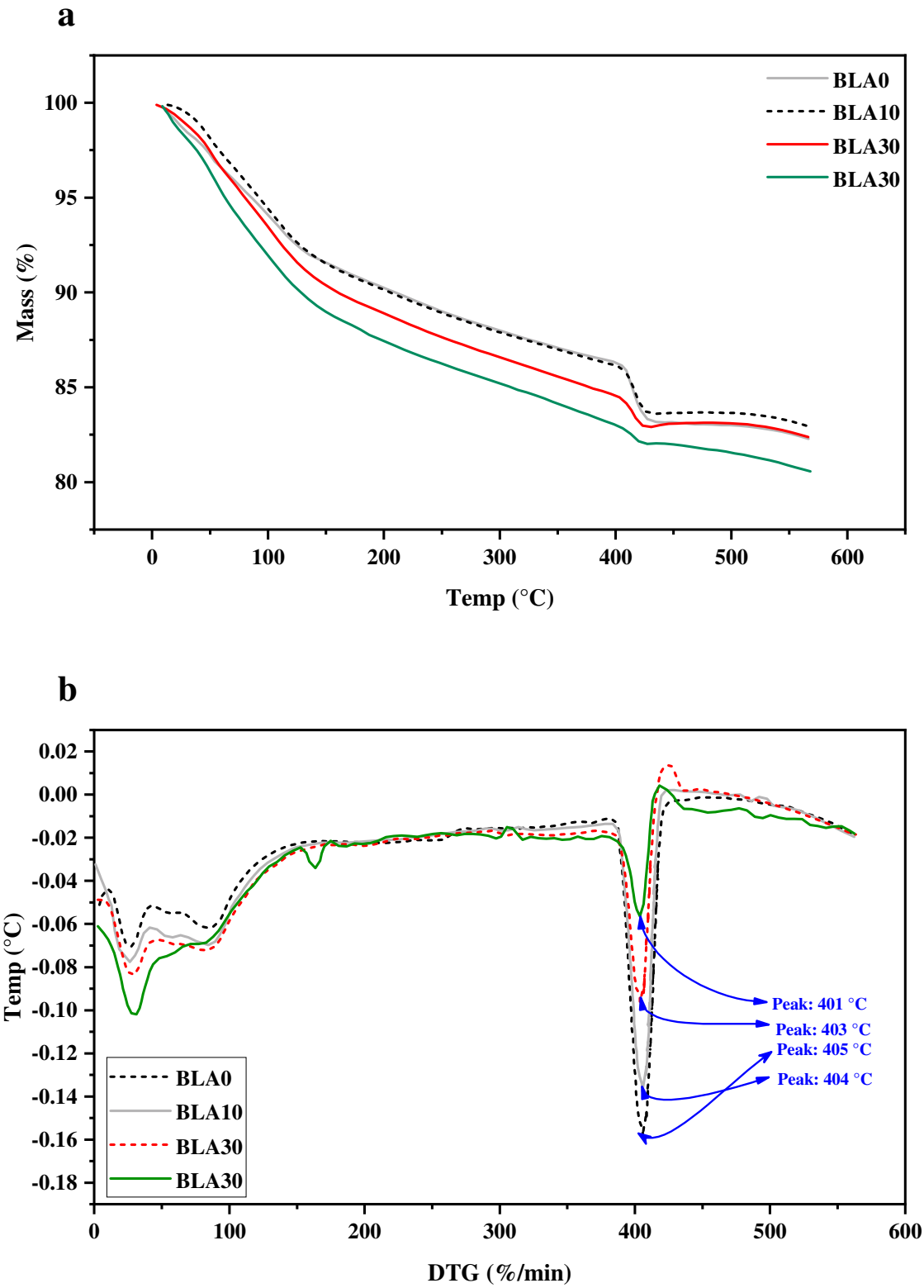

Figure 26. (a) TGA and (b) DTG of BLA based morters.

The derivative thermogravimetry (DTG) and thermogravimetric analysis (TGA) findings of Banana leaf ash-based mortars in the temperature range of 30 °C to 580 °C are shown in Figure 26. The decrease in mass that was observed across all of the samples was caused by the gradual increase in temperature. Due to the fact that free water evaporated at 100 degrees Celsius, the mass loss in TG between 100 degrees Celsius and 580 degrees Celsius was taken into consideration as a measurement of total mass loss. According to Figure 26-a, the BLA30 mixture exhibited the highest mass loss percentage, whereas the BLA0 mixture exhibited the lowest mass loss percentages. On the other hand, in comparison to the reference mix, the BLA10 and BLA20 mix displayed slightly higher amount of mass loss. This can be attributable to the increased water demand of fresh BLA samples; this water accumulates in pores larger than 5 nm [55]. The weight loss in TGA data above 300 °C is attributed to dehydration of chemically bonded water [56] and an increase in geopolymer reaction products [57].

According to the results of the DTG, the highest peak temperatures were recorded at 405 °C for the BLA0 mix, 404 °C for the BLA10 mix, 403 °C for the BLA20 mix, and 401 °C for the BLA30 mix. The peak temperature for all mixtures was nearly identical, with the exception of the BLA0 mix, for which it shifted upwards relative to BLA30 mix. The trend is influenced by the Portlandite that has developed in the paste due to the hydration of free lime. Among the phases that critically influence the performance of a cement-based material is $Ca(OH)_2$, of which the crystalline variant is known as portlandite. Portlandite is quantitatively the most important crystalline hydration product, which is known to affect the durability and corrosion resistance of concrete [58]. This corresponds nicely with the amount of free lime in the dehydrated ash [59].

3.5. Microstructural analysis

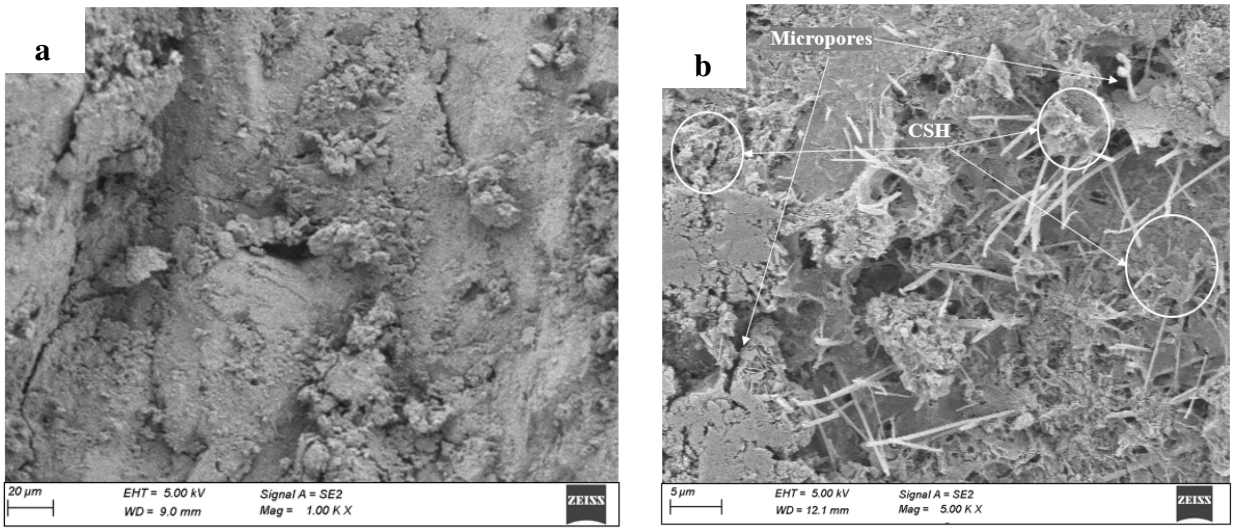

Figure 27: SEM image of (a) BLA0 mix and (b) BLA30 mix at 28 days.

Figure 27-a demonstrates that the microstructural property of control specimen after 28 curing days appears to be denser and contains minimal amounts of calcium hydroxide (CH) and ettringite content. In addition, Figure 27-b shows how the BLA specimens appear to form a net like structural appearance, which most likely suggests the presence of secondary CSH. According to the TGA analysis of the specimens, it also reveals a negligible quantity of CH, also known as higher brightness crystal (mass loss and small melting curve). In addition, the microstructure of the BLA specimens reveals a significant quantity of ettringite production, which may be explained by the presence of aluminum oxide (Al_2O_3). However, the BLA specimens exhibited greater microcracks than the control specimen, which led to the loss of strength and the high chloride ion penetration rate.

3.6. Environmental Impact and Cost Benefit Assessment

Cement production accounts for around 10 percent of worldwide CO_2 emissions [60-62]. Due to the activities involved in preparing raw materials, concrete, the world's most widely used building material, has a substantial carbon footprint. Since OPC is the primary binding material of concrete, it is responsible for between 75 and 90 percent of the total CO_2 emissions [62] produced by concrete. The awareness of Global Warming Potential ($kgCO_2$-eq/kg material) has enabled the development of alternative binders to reduce concrete's reliance on OPC as its primary binder.

Table 9. CO_2 emissions data for concrete

Materials	Emission (kg-CO_2/kg)	Reference
OPC	0.93	[63]
BLA	0	[63]
Sand	0.005	[63]
Stone Chips	0.0409	[64]
Water	0.000196	[65]
Superplasticizer	0.720	[66]

Although using SCMs will undoubtedly lower the overall embodied CO_2 emissions of concrete, the embodied CO_2 emissions of different waste materials will vary. Regarding the present investigation, BLA was partially utilized as a binder to replace OPC. To highlight the impact of BLA on the overall embedded CO_2 emissions of SCC, this study estimates the total

CO_2 emissions considering the equivalent CO_2 releases for each material. These numbers were extracted from relevant research studies and are presented in Table 9.

The embodied GWP for each mixture was calculated by multiplying the weight of each ingredient required to manufacture one cubic meter of concrete by the embodied CO_2 of each material and then adding the results. From Figure 28, the OPC has the highest CO_2 content compared to other materials. OPC is responsible for roughly 89.10 percent of the total CO_2 emissions for the Control mix (BLA0). This was significantly reduced by substituting 30% OPC with BLA (BLA30 mix). For BLA30 mix, the CO_2 contribution of OPC input decreased from 478.82 to 339.6 kg-CO_2/m^3. In addition, BLA10, BLA20 reduced 9.71% and 19.42% of CO_2 emissions, respectively.

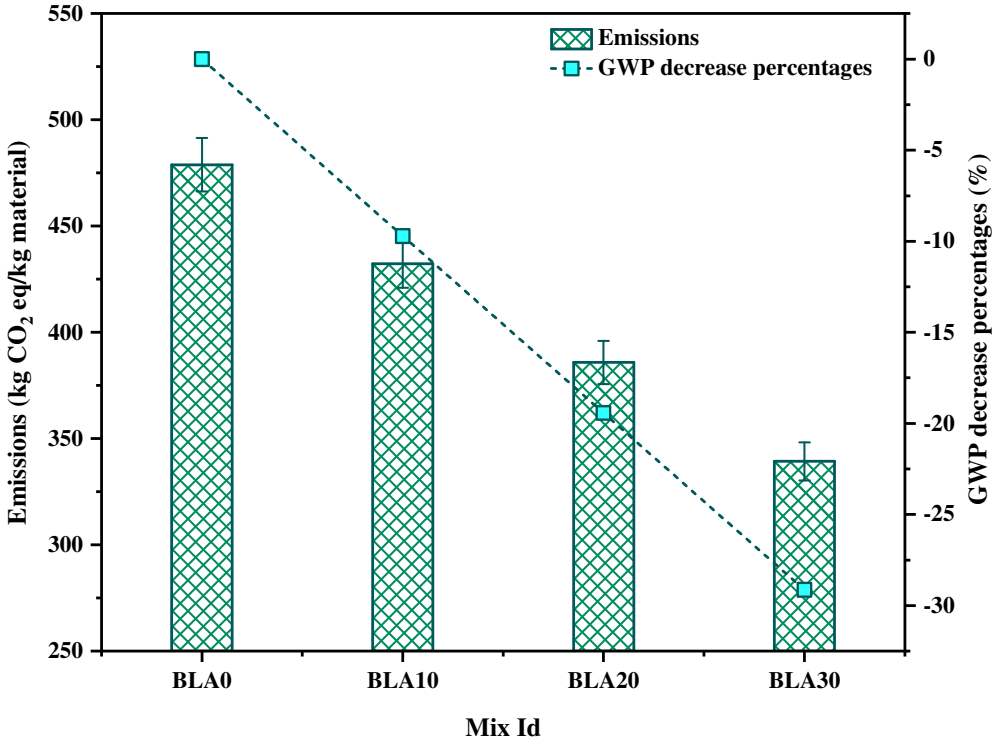

Figure 28. Total CO_2 emission and GWP enhancement percentage

The eco-strength efficiency of concrete is another metric that may be applied to the environmental impact assessment for evaluation. Alnahhal et al. [67] used the term eco-strength efficiency, which Damineli et al. [68] referred to as the CO_2 intensity, which can be defined as the quantity of CO_2 emissions produced per unit of performance. It was determined using Equation (5)

$$C_i = \frac{CO_2}{C_s} \quad (5)$$

where C_i represents the eco-strength efficiency, which is the intensity of CO_2, CO_2 represents the embodied Carbon dioxide emissions released by the concrete mixes as determined using Table 10, and C_s represents the compressive strength.

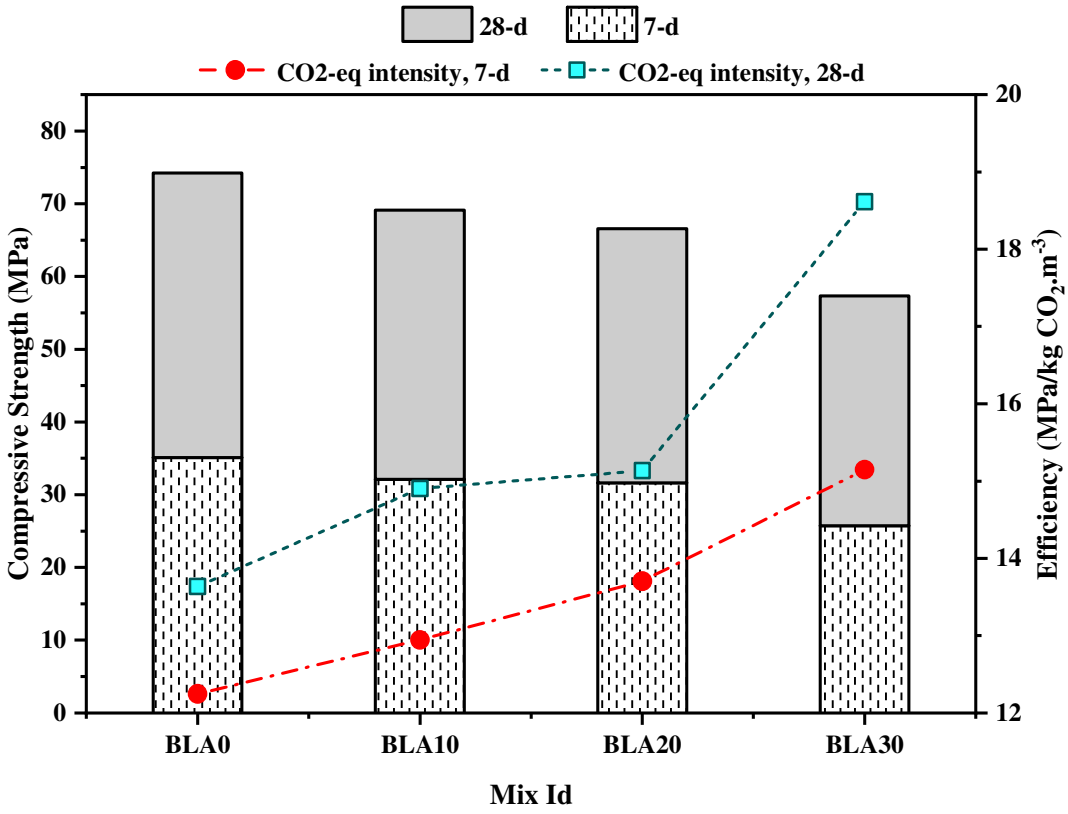

Figure 29. Eco-strength efficiency with respect to compressive strength.

The eco strength efficiency of the various mixes is compared with their compressive strength to facilitate an organized and consistent comparison of the mixes. Figure 29 depicts the results of the study. The compressive strength values for 7 and 28 days are represented by the bar chart from bottom to top, while the CO_2 intensity is represented by the line along the secondary axis. The CO_2 intensity allows for the evaluation of both performance and contribution of concrete mixes to Global Warming Potential per their unit strength, which makes it a good predictor of the impact of concrete use [68]. In most cases, the concentration of CO_2 rises when there is a greater amount of Portland cement in the concrete mixture. Substituting cement with BLA, CO_2 intensity can be reduced for a given strength, particularly

at later ages. For instance, lowering the percentage of Portland cement from 100% (BLA0) to 30% (BLA30) enhances the efficiency from 13.53 MPa/kgCO_2-eq.m^{-3} to 18.61 MPa/kgCO_2-eq.m^{-3}.

3.7. Cost Analysis

Table 10. Local prices of the materials

Materials	Cement	BLA	Sand	Stone chips	Water	Superplasticizer
Cost ($/kg)	0.142	0.0009	0.024	0.071	0.0006	2.36

Prior to implementing any new or mixed concrete, the construction industry considers the environmental impact assessment and cost-benefit analysis to be two of the most important criteria. The cost-benefit analysis of concrete, which was the subject of this study, was computed for each mix based on the costs of the individual materials in the area. Table 10 displays, in US Dollars, the cost of one kilogram of each commodity when converted from BDT (1 USD = 93 BDT). The availability of various materials in a given region significantly impacts their respective pricing. Because of this, the price of BLA, a pozzolanic material, is considerably less than the cost of OPC. Figure 19-a depicts the cost of each concrete mixture per 1 cubic meter. It can be seen that the BLA0 mix has a price of $149.56 per m^3 of concrete. The OPC and the Superplasticizer are the primary factors that determine the pricing. The BLA30 mix has the lowest overall cost, costing $130.49 per m^3 of concrete produced. Compared to the control mix, this is approximately 12.74 percent less expensive.

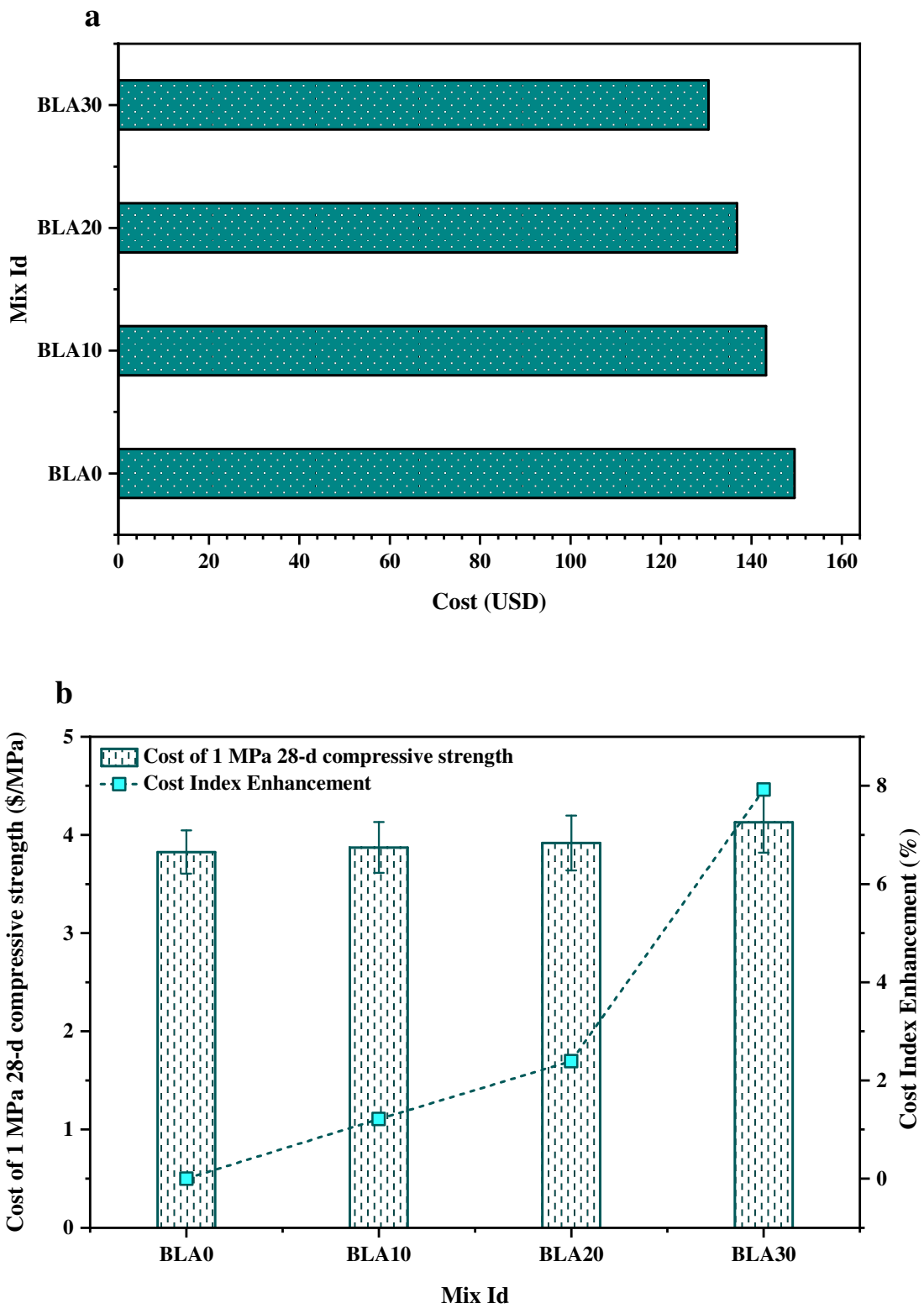

Figure 30. (a) Cost analysis of 1 m^3 concrete mixes (b) Cost index of the mixes.

Figure 30-a shows that the overall cost of each mix varies; however, a definitive cost-benefit analysis cannot be regarded adequate without examining the cost of producing 1 MPa of

strength for each mix. Figure 30-b illustrates the resulting cost to manufacture a 1-MPa compressive strength at 28 days, which can be referred as cost index of the mixes. The lowest cost of producing 1 MPa was exhibited by BLA0 mix of 3.82 $/MPa. The BLA10, BLA20, and BLA30 mixes, on the other hand, showed cost indexes of 3.87, 3.91, and 4.12 $/MPa, respectively, with an increase of 1.21, 2.39, and 7.9% over the control mix. The control mix clearly had the lowest cost index, but the addition of BLA did not considerably increase the cost index of the produced mixes.

Conclusions

In this investigation, the fresh, hardened, microstructural, and environmental effects of BLA-based cementitious composites are studied. The critical outcomes of this experimental investigation are concluded below:

- The outcome of all mixes was within the EFNARC range, even though the fresh concrete's workability decreased as the BLA concentration increased. Instead of BLA's high water demand at fresh state, all the mixes depicted sufficient workability, passing ability, and flow ability with an improved viscosity.
- Despite a declining pattern in the strength parameters of the BLA-incorporated samples, mixes containing up to 20% BLA demonstrated nearly equal mechanical and durability characteristics compared to the control mix. Therefore, up to 20% BLA can be substituted in SCC as supplementary cementing material.
- Concrete containing BLA-blended binders up to 20% can attain comparable resistance versus chemical attack. At 28 days, the mixture with 20% BLA exhibited roughly 4% greater chloride ion penetration than the control mix. In terms of water permeability, the permeability coefficient increased by only 0.27 ms^{-1} for 20% BLA at 56 days.
- In terms of microstructural properties, ettringite formation was observed for the BLA blended mixes.
- The findings of the thermogravimetric (TGA and DTG) analysis showed that greater temperatures were necessary to disintegrate the configuration of the cementitious paste when the BLA was incorporated. BLA10, BLA20, and BLA30 required more heat energy to evaporate water compared to BLA0.

- BLA30 depicted the lowest GWP of 339 kgCO2-eq/kg material, with a 29.13% reduction than the control mix, whereas the BLA20 mix represented an 19.41% GWP reduction demonstrating a significant eco-strength efficiency.

- In terms of cost–benefit analysis, the BLA30 mix had the lowest overall cost, projected to be approximately 4.12% less expensive than the control mix. Although the BLA20 mix showed little cost reduction (only 3.87% than the control mix), it depicted the cost index value of 3.91 USD/MPa, which is almost identical to the control mix.

Acknowledgements

The authors would like to thank Bashundhara Cement, Bangladesh for providing cement. The authors would also like to pay gratitude to all the lab technicians of the Structural and Materials Engineering Laboratory from Khulna University of Engineering & Technology and The Centre for Sophisticated Instrumentation and Research Laboratory from Jashore University of Science and Technology. Finally, the authors would like to express their gratitude to two anonymous reviewers, whose insightful comments significantly contributed to the manuscript's overall improvement.

References

[1] K. Prasad, V. Vasugi, R. Venkatesan, N.S. Bhat, Critical causes of time overrun in Indian construction projects and mitigation measures, International Journal of Construction Education and Research 15(3) (2019) 216-238.

[2] A.S. Gill, R.J.C. Siddique, B. Materials, Durability properties of self-compacting concrete incorporating metakaolin and rice husk ash, 176 (2018) 323-332.

[3] H. Nouri, M. Safehian, S.M.M.M. Hosseini, Life cycle assessment of earthen materials for low-cost housing a comparison between rammed earth and fired clay bricks, International Journal of Building Pathology and Adaptation (2021).

[4] A.C.P. Martins, J.M.F. de Carvalho, L.C.B. Costa, H.D. Andrade, T.V. de Melo, J.C.L. Ribeiro, L.G. Pedroti, R.A.F. Peixoto, Steel slags in cement-based composites: An ultimate review on characterization, applications and performance, Construction and Building Materials 291 (2021) 123265.

[5] G. Fayomi, S. Mini, O. Fayomi, A. Ayoola, Perspectives on environmental CO2 emission and energy factor in Cement Industry, IOP Conference Series: Earth and Environmental Science, IOP Publishing, 2019, p. 012035.

[6] A. Pakdel, H. Ayatollahi, S. Sattary, Embodied energy and CO2 emissions of life cycle assessment (LCA) in the traditional and contemporary Iranian construction systems, Journal of Building Engineering 39 (2021) 102310.

[7] M. Sahmaran, A. Yurtseven, I.O.J.B. Yaman, Environment, Workability of hybrid fiber reinforced self-compacting concrete, 40(12) (2005) 1672-1677.

[8] H. Okamura, M.J.J.o.a.c.t. Ouchi, Self-compacting concrete, 1(1) (2003) 5-15.

[9] R. Hasan, M.H.R. Sobuz, A.S.M. Akid, M.R. Awall, M. Houda, A. Saha, M.M. Meraz, M.S. Islam, N.M. Sutan, Eco-friendly self-consolidating concrete production with reinforcing jute fiber, Journal of Building Engineering (2022) 105519.

[10] Y. Khodair, B.J.C. Bommareddy, B. Materials, Self-consolidating concrete using recycled concrete aggregate and high volume of fly ash, and slag, 153 (2017) 307-316.

[11] ACI Committee 237, ACI Manual of Concrete Practice, ACI 237R-07, Detroit, MI. (2007).

[12] M. Şahmaran, İ.Ö. Yaman, M.J.C. Tokyay, c. composites, Transport and mechanical properties of self consolidating concrete with high volume fly ash, 31(2) (2009) 99-106.

[13] T.R. Naik, Singh, S. S., & Hossain, M. M, Permeability of high-strength concrete containing low cement factor, Journal of energy engineering 122(1) (1996) 21-39.

[14] N. Makul, Combined use of untreated-waste rice husk ash and foundry sand waste in high-performance self-consolidating concrete, Results in Materials 1 (2019) 100014.

[15] A. Adesina, P. Awoyera, Overview of trends in the application of waste materials in self-compacting concrete production, SN Applied Sciences 1(9) (2019) 1-18.

[16] J.P. Moretti, S. Nunes, A. Sales, Self-compacting concrete incorporating sugarcane bagasse ash, Construction and Building Materials 172 (2018) 635-649.

[17] R.K. Sandhu, R. Siddique, Properties of sustainable self-compacting concrete made with rice husk ash, European Journal of Environmental and Civil Engineering (2021) 1-25.

[18] M. Sathurshan, I. Yapa, J. Thamboo, T. Jeyakaran, S. Navaratnam, R. Siddique, J. Zhang, Untreated rice husk ash incorporated high strength self-compacting concrete:

Properties and environmental impact assessments, Environmental Challenges 2 (2021) 100015.

[19] M.H.R. Sobuz, A. Saha, J.F. Anamika, M. Houda, M. Azab, A.S.M. Akid, M.J. Rana, Development of Self-Compacting Concrete Incorporating Rice Husk Ash with Waste Galvanized Copper Wire Fiber, Buildings 12(7) (2022) 1024.

[20] K.A. Thammaiah, P.M. Prasad, C. Nishchel, R.S. Ballavur, Y. Rohith, Self-compacting Concrete Using Tobacco Waste Ash, Recent Advances in Civil Engineering: Proceedings of the 2nd International Conference on Sustainable Construction Technologies and Advancements in Civil Engineering (ScTACE 2021), Springer Nature, 2022, p. 1.

[21] M.Z. Syahmi, W.I. Goh, Long-Term Behavior of Self-Compacting Concrete Incorporating Palm Oil Fuel Ash and Eggshell Powder as Partial Cement Replacement, Recent Trends in Civil Engineering and Built Environment 3(1) (2022) 104-112.

[22] ASTM-C125, Standard terminology relating to concrete and concrete aggregates., ASTM International, West Conshohocken, PA. (2013).

[23] B.S. Thomas, J. Yang, K.H. Mo, J.A. Abdalla, R.A. Hawileh, E. Ariyachandra, Biomass ashes from agricultural wastes as supplementary cementitious materials or aggregate replacement in cement/geopolymer concrete: A comprehensive review, Journal of Building Engineering 40 (2021) 102332.

[24] G.d.S. S Junior, M.B.d. Morais, T.R. Camara, L.J.R.B.d.E.A.e.A. Willadino, Growth of dipoid banana genotypes under saline stress, 16 (2012) 1145-1151.

[25] G. Aurore, B. Parfait, L.J.T.i.F.S. Fahrasmane, Technology, Bananas, raw materials for making processed food products, 20(2) (2009) 78-91.

[26] R.C. Kanning, Utilização da cinza de folha de bananeira como adição de argamassas de cimento Portland, (2013).

[27] R.C. Kanning, K.F. Portella, M.O. Bragança, M.M. Bonato, J.C. dos Santos, Banana leaves ashes as pozzolan for concrete and mortar of Portland cement, Construction and Building Materials 54 (2014) 460-465.

[28] R. Kanning, K. Portella, M. Costa, R. Puppi, Evaluation of pozzolanic activity of banana leaf ash, International Conference on Durability of Building Materials and Components, Porto, Portugal, 2011.

[29] BS EN 197-1, Cement - Part 1: Composition, specifications and conformity criteria for common cements, British Standards Institution, London, UK, 2011.

[30] A.G. Vayghan, A. Khaloo, F. Rajabipour, The effects of a hydrochloric acid pre-treatment on the physicochemical properties and pozzolanic performance of rice husk ash, Cement and Concrete Composites 39 (2013) 131-140.

[31] ASTM C618, Standard Specification for Coal Fly Ash and Raw or Calcined Natural Pozzolan for Use in Concrete, ASTM International, West Conshohocken, PA, 2018.

[32] ASTM C136 / C136M-19, Standard Test Method for Sieve Analysis of Fine and Coarse Aggregates, ASTM International, West Conshohocken, PA, 2019.

[33] ASTM C494/C494M-08, Standard Specification for Chemical Admixtures for Concrete, ASTM International, West Conshohocken, PA, 2008.

[34] I. 10262, Concrete mix proportioning-guidelines, Indian Standard Code (2009).

[35] EFNARC, Specifications and Guidelines for Self-Compacting Concrete,, EFNARC Publication London, 2002, pp. 1–32.

[36] BS EN 12350-8, Testing Fresh Self-compacting Concrete. Slump flow test., British Standards Institution, London, UK, 2010b.

[37] BS EN 12350-10, Testing fresh concrete Self-compacting concrete. L box test, British Standards Institution, London, UK, 2010.

[38] BS EN 12350-12, Testing fresh concrete Self-compacting concrete. J-ring test, British Standards Institution, London, UK, 2010.

[39] ASTM-C39/C39M-18, Standard test method for compressive strength of cylindrical concrete specimens., ASTM International, West Conshohocken, PA, 2018.

[40] ASTM-C496, Standard Test Method for Splitting Tensile Strength of Cylindrical Concrete Specimens, ASTM International, West Conshohocken, PA. (2018).

[41] ASTM-C78/C78M-18, Standard test method for flexural strength of concrete (using simple beam with Third-Point loading). , ASTM International, West Conshohocken, PA, 2018.

[42] ASTM-C1202, Standard Test Method for Electrical Indication of Concrete's Ability to Resist Chloride Ion Penetration, ASTM International, West Conshohocken, PA. (2019).

[43] ASTM-C642, Standard Test Method for Density, Absorption, and Voids in Hardened Concrete, ASTM International, West Conshohocken, PA. (2021).

[44] T. Akram, S.A. Memon, H. Obaid, Production of low cost self compacting concrete using bagasse ash, Construction and Building Materials 23(2) (2009) 703-712.

[45] D. Chopra, R. Siddique, Strength, permeability and microstructure of self-compacting concrete containing rice husk ash, Biosystems engineering 130 (2015) 72-80.

[46] J.C. Tavares, L.F. Lucena, G.F. Henriques, R.L. Ferreira, M.A. dos Anjos, Use of banana leaf ash as partial replacement of Portland cement in eco-friendly concretes, Construction and Building Materials 346 (2022) 128467.

[47] ASTM-C1621/C1621M, Standard Test Method for Passing Ability of Self-Consolidating Concrete by J-Ring, ASTM International, West Conshohocken, PA. (2019).

[48] R. Vignesh, R.R. Nevas, S. Ruban, C. Ramesh, B. Gowtham, Experimental Study on Slump and Strength Properties of Concrete by Replacement of Cement Using Banana Leaf Ash, The Journal of Solid Waste Technology and Management 47(3) (2021) 482-486.

[49] J.R. Pawar, S.K. Aman, Experimental investigation on properties of concrete by partial replacement of cement with banana leaves ash, Proceedings of the 6th International Conference on Recent Trends in Engineering & Technology (ICRTET-2018), 2018.

[50] O.I. Ndubuisi, Potentials of banana leaf ash as admixture in the production of concrete

[51] ASTM-C109/C109M-20, Standard Test Method for Compressive Strength of Hydraulic Cement Mortars (Using 2-in. or [50-mm] Cube Specimens). ASTM International., West Conshohocken, PA, 2020.

[52] ACI-318, Building code requirements for structural concrete (ACI 318-99) and commentary (318R-99), American Concrete Institute., Farmington Hills, MI, 2008.

[53] ASTM-C1202-19, Standard Test Method for Electrical Indication of Concrete's Ability to Resist Chloride Ion Penetration., ASTM International, West Conshohocken, PA, 2019.

[54] V. Kannan, K. Ganesan, Chloride and chemical resistance of self compacting concrete containing rice husk ash and metakaolin, Construction and Building Materials 51 (2014) 225-234.

[55] F. Škvára, L. Kopecký, V. Šmilauer, Z. Bittnar, Material and structural characterization of alkali activated low-calcium brown coal fly ash, Journal of hazardous materials 168(2-3) (2009) 711-720.

[56] R.D. Recommendation, P. De La Rilem, 129-MHT: test methods for mechanical properties of concrete at high temperatures, Materials and Structures 28 (1995) 410-414.

[57] S. Nath, S. Maitra, S. Mukherjee, S. Kumar, Microstructural and morphological evolution of fly ash based geopolymers, Construction and Building Materials 111 (2016) 758-765.

[58] L. Bertolini, B. Elsener, P. Pedeferri, E. Redaelli, R.B. Polder, Corrosion of steel in concrete: prevention, diagnosis, repair, John Wiley & Sons2013.

[59] P. Chindaprasirt, U. Rattanasak, Utilization of blended fluidized bed combustion (FBC) ash and pulverized coal combustion (PCC) fly ash in geopolymer, Waste Management 30(4) (2010) 667-672.

[60] Y.J. Zhang, S. Li, Y.C. Wang, Microstructural and strength evolutions of geopolymer composite reinforced by resin exposed to elevated temperature, Journal of Non-Crystalline Solids 358(3) (2012) 620-624.

[61] B. Suhendro, Toward green concrete for better sustainable environment, Procedia Engineering 95 (2014) 305-320.

[62] R. Kumar, N. Shafiq, A. Kumar, A.A. Jhatial, Investigating embodied carbon, mechanical properties, and durability of high-performance concrete using ternary and quaternary blends of metakaolin, nano-silica, and fly ash, Environmental Science and Pollution Research 28(35) (2021) 49074-49088.

[63] J.T. Kolawole, K.O. Olusola, A.J. Babafemi, O.B. Olalusi, E. Fanijo, Blended cement binders containing bamboo leaf ash and ground clay brick waste for sustainable concrete, Materialia 15 (2021) 101045.

[64] L.K. Turner, F.G. Collins, Carbon dioxide equivalent (CO2-e) emissions: A comparison between geopolymer and OPC cement concrete, Construction and building materials 43 (2013) 125-130.

[65] K.-H. Yang, J.-K. Song, K.-I. Song, Assessment of CO2 reduction of alkali-activated concrete, Journal of Cleaner Production 39 (2013) 265-272.

[66] G. Long, Y. Gao, Y. Xie, Designing more sustainable and greener self-compacting concrete, Construction and Building Materials 84 (2015) 301-306.

[67] M.F. Alnahhal, U.J. Alengaram, M.Z. Jumaat, F. Abutaha, M.A. Alqedra, R.R. Nayaka, Assessment on engineering properties and CO2 emissions of recycled aggregate concrete incorporating waste products as supplements to Portland cement, Journal of cleaner production 203 (2018) 822-835.

[68] B.L. Damineli, F.M. Kemeid, P.S. Aguiar, V.M. John, Measuring the eco-efficiency of cement use, Cement and Concrete Composites 32(8) (2010) 555-562.